



Science & Global Security

The Technical Basis for Arms Control, Disarmament, and
Nonproliferation Initiatives

ISSN: (Print) (Online) Journal homepage: www.tandfonline.com/journals/gsgs20

Hypersonic Weapons: Vulnerability to Missile Defenses and Comparison to MaRVs

David Wright & Cameron L. Tracy

To cite this article: David Wright & Cameron L. Tracy (2023) Hypersonic Weapons: Vulnerability to Missile Defenses and Comparison to MaRVs, *Science & Global Security*, 31:3, 68-114, DOI: [10.1080/08929882.2023.2270292](https://doi.org/10.1080/08929882.2023.2270292)

To link to this article: <https://doi.org/10.1080/08929882.2023.2270292>



View supplementary material [↗](#)



Published online: 24 Oct 2023.



Submit your article to this journal [↗](#)



Article views: 1083



View related articles [↗](#)




View Crossmark data [↗](#)



Citing articles: 4 View citing articles [↗](#)



Hypersonic Weapons: Vulnerability to Missile Defenses and Comparison to MaRVs

David Wright^a and Cameron L. Tracy ^b

^aLaboratory for Nuclear Security and Policy, Department of Nuclear Science and Engineering, Massachusetts Institute of Technology, Cambridge, MA, USA; ^bCenter for International Security and Cooperation (CISAC), Freeman Spogli Institute for International Studies, Stanford University, Stanford, CA, USA

ABSTRACT

Assessing the utility of hypersonic boost glide vehicles (BGVs) requires comparing their capabilities to alternative systems that could carry out the same missions, particularly given the technical difficulties and additional costs of developing BGVs compared to more established technologies. This paper discusses the primary motivations given for BGVs—most notably countering missile defenses—and summarizes current hypersonic development programs. It finds that evading the most capable current endo-atmospheric defenses requires that BGVs maintain speeds significantly higher than Mach 5 throughout their glide phase, which has implications for their mass and range. The paper then compares BGVs to maneuverable reentry vehicles (MaRVs) carried on ballistic missiles flown on depressed trajectories and shows that MaRVs can offer significant advantages over BGVs in a wide range of cases. Finally, the paper shows that BGV maneuvering during its glide phase can result in substantial costs in range and glide speed.



ARTICLE HISTORY


Received 3 February 2023
Accepted 5 September 2023

The United States, Russia, and China are leading the development of hypersonic weapons: vehicles primarily intended to glide for long distances within the atmosphere at speeds greater than five times the speed of sound, or Mach 5.¹ Several other nations have smaller active development programs.²

Assessing hypersonic vehicles requires understanding what capabilities they may provide compared to alternative systems that could carry out the same missions, particularly given the technical difficulties and additional costs of developing hypersonic gliders compared to more established technologies.

In particular, we compare hypersonic glide weapons to maneuverable reentry vehicles (MaRVs) carried on ballistic missiles flown on depressed trajectories (DTs).³ DTs are ballistic trajectories with significantly smaller

CONTACT David Wright  dcwright@mit.edu  Laboratory for Nuclear Security and Policy, Department of Nuclear Science and Engineering, Massachusetts Institute of Technology, Cambridge, MA, 02139, USA.

 Supplemental data for this article can be accessed online at <https://doi.org/10.1080/08929882.2023.2270292>.

This article has been corrected with minor changes. These changes do not impact the academic content of the article.

© 2023 Taylor & Francis Group, LLC

loft angles, and therefore lower apogees and shorter trajectory lengths for a given ground range, than those trajectories that maximize missile range. MaRVs use atmospheric forces to maneuver during the terminal phase of flight and can provide many of the capabilities motivating hypersonic weapon development. In particular, the ability to maneuver during reentry could allow MaRVs to evade terminal defenses, to use terminal guidance for high accuracy, to retarget over hundreds of kilometers, and to dive to targets at a steep angle. Unlike hypersonic gliders, MaRVs cannot maneuver significantly during midcourse flight or fly for long distances at altitudes below 50 km, and do not glide to substantially increase their flight ranges.

Our previous paper, referred to here as Paper 1,⁴ analyzed hypersonic weapon performance using a computational model of hypersonic flight and vehicle parameters derived from tests of the U.S. Hypersonic Technology Vehicle-2 (HTV-2), a representative glider, conducted in 2010 and 2011.⁵ We assessed common assertions made about hypersonic weapons with regard to delivery time, maneuverability, and detectability, finding that many of these claims were exaggerated or false.

Paper 1 focused on long-range hypersonic vehicles, like the HTV-2 and the Russian Avangard (Vanguard).⁶ Both systems are said to reach speeds of Mach 20 or higher.⁷

After testing the HTV-2, U.S. focus shifted from intercontinental missiles to shorter-range, lower-speed systems (with non-nuclear warheads). The analysis in Paper 1 also applied to shorter-range hypersonic weapons, but here we consider those systems more specifically—in particular, hypersonic vehicles with ranges up to a few thousand kilometers and speeds of Mach 5–12.

Since ballistic missiles with ranges of more than a few hundred kilometers reach hypersonic speeds, the term “hypersonic weapons” is ambiguous. We instead refer to weapons that travel a significant portion of their trajectories at low altitudes, relying primarily on lift forces to stay aloft, as “hypersonic boost glide vehicles” (BGVs). BGVs are accelerated to high speed by rocket boosters and then glide without power to their targets. In addition, there are hypersonic cruise missiles (HCMs), which also use boosters to reach hypersonic speed and rely on lift forces to reach long distances but carry engines to maintain their speed throughout flight.

In this paper, we discuss the primary motivations given for developing hypersonic weapons and summarize the evolution and current status of U.S. BGV programs, then look in detail at three topics:

1. The capability of current missile defense systems to intercept hypersonic weapons. We show that evading defenses appears to require that BGVs

- maintain speeds throughout their glide phases significantly greater than Mach 5.
2. A comparison of ranges, masses, and flight times of BGVs and MaRVs under various conditions, including when the BGV speed is high enough to evade defenses. This analysis shows that MaRVs out-perform BGVs in many scenarios.
 3. An analysis of the midcourse maneuvering capability of BGVs, which is cited as an advantage of BGVs over MaRVs. We show that this maneuvering can result in a significant reduction of speed and range.

Motivations for hypersonic weapons

Advocates of BGVs discuss a broad set of motivations for developing them; we list key motivations below.⁸ There is little discussion, however, of which motivations can uniquely, or even best, be fulfilled by BGVs, and therefore whether these motivations justify the efforts and expenditure needed to solve the difficult technical challenges facing BGVs.⁹ In other words, do BGVs offer meaningful advantages over systems such as ballistic missiles with MaRVs?

The primary motivations given by those leading U.S. BGV development are:¹⁰

1. To quickly attack targets from long ranges
2. To achieve high accuracies and home on targets (which requires terminal maneuvering)
3. To retarget over a large area during flight (which requires terminal and/or midcourse maneuvering)
4. To evade or destroy air defenses and missile defenses.¹¹

If the aim is to accomplish goals (1)–(4), there are several types of weapons that could do so.

For example, these goals do not require flying low in the atmosphere for long distances and could instead be met by ballistic missiles with MaRVs. MaRVs have the significant advantage that they rely largely on existing technology, and therefore present fewer technical challenges and may therefore have higher reliability and lower cost than BGVs and HCMs. A 2023 report by the Congressional Budget Office states that MaRVs and BGVs would have similar capabilities in a conflict, but that BGVs “could cost one-third more to procure and field than ballistic missiles of the same range with maneuverable warheads.”¹²

We show in Paper 1 that MaRVs launched on DTs can have shorter delivery times than BGVs because they encounter less drag.¹³ This means

that the desire for hypersonic speed and short delivery time does not argue uniquely for BGVs.

Both BGVs and MaRVs can maneuver during the terminal phase and could be equipped with a similar ability to home on targets. Terminal maneuvering also allows both systems to retarget by hundreds of kilometers. While MaRVs cannot maneuver significantly during the midcourse phase, below we show that midcourse maneuvering by BGVs can result in a significant reduction of speed and range and therefore may not offer a particular advantage over the maneuvering offered by MaRVs.

Moreover, if significant maneuvering is seen as crucial for a given mission, then developing supersonic cruise missiles may be a better choice than BGVs and would face fewer technical hurdles. A supersonic vehicle traveling at Mach 3 would be subjected to a heating rate during its glide phase that is roughly eight times smaller than a hypersonic vehicle traveling at Mach 6, since atmospheric heating, which is a major impediment to developing BGVs, increases approximately with the cube of velocity.

Finally, we compare below the ability of BGVs and MaRVs to evade missile defenses.

This paper compares the capabilities of BGVs and ballistic missiles with MaRVs designed to reach distances of up to a few thousand kilometers and speeds of Mach 5–12. While HCMs are not considered in detail, our models apply to analysis of these systems as well. We show that comparing the capabilities of these systems requires specifying the mission they are intended to carry out, the launch platform, the need to evade defenses, and other parameters.

Comparing BGVs with MaRVs

BGVs and MaRVs are not entirely distinct means of delivering warheads. Both are accelerated by booster rockets and typically have a ballistic phase for some period after booster burnout. A MaRV's ballistic phase will make up most of its trajectory, continuing until it reenters the atmosphere. A BGV of the same range will follow a shorter ballistic phase before beginning its glide phase. For the BGVs considered here, the glide phase typically makes up about half of the weapon's total range.¹⁴ To exit from glide as it approaches its target, a BGV uses aerodynamic forces to dive to the ground.

A standard ballistic missile reentry vehicle relies on inertial forces due to its high speed to stay aloft during its long ballistic phase, while gliders sacrifice some speed to drag but stay aloft for a significant portion of flight using lift forces, by traveling at lower altitudes. MaRVs represent a middle ground, flying much of their trajectory ballistically, then using lift forces to

maneuver late in flight. A MaRV might be considered a hypersonic glider that reenters the atmosphere relatively late in flight. Both MaRVs and BGVs follow non-ballistic trajectories for part of their flight.

For very long-range systems, a BGV spends a much larger fraction of its trajectory within the atmosphere than does a ballistic missile with a MaRV. For example, the full test range for the U.S. HTV-2 flight tests was about 7,600 km. The glider was intended to travel about 75% of that distance at altitudes below 100 km (generally considered to be the upper edge of the atmosphere) and about 60% gliding below 50 km.¹⁵ In contrast, a MaRV on a long-range trajectory would spend well under 10% of its trajectory below 50 km.

For shorter ranges, the distinction is less clear. The apogee of an efficient ballistic missile trajectory decreases with its maximum range, so for shorter-range systems the reentry vehicle will spend more of its trajectory within the atmosphere. A warhead on a 10,000 km-range “minimum-energy” trajectory (MET) will reach altitudes of about 1,500 km.¹⁶ Missiles on METs with ranges less than 400 km never leave the atmosphere (the apogee of a short-range missile on an MET is about a quarter of its range). In addition, ballistic missiles flown on less energy-efficient depressed trajectories can use a more powerful booster to reach the same range as a warhead following an MET, but with a lower apogee due to their higher initial speed.¹⁷

A potential advantage of gliding is that by using lift forces to stay aloft a BGV can reach a given range with a lower initial speed than a ballistic missile warhead and could therefore require a smaller booster to accelerate it. Booster technology, however, is well developed and building a somewhat larger booster to deliver a ballistic missile warhead is often feasible. Smaller boosters could be an advantage for air-launched vehicles since they would reduce the mass the aircraft needs to carry; they could also be useful for vehicles launched from submarines where space is restricted.

The fuzziness in the distinction between MaRVs and BGVs is apparent in the history of U.S. development efforts, discussed below.¹⁸

Evolution of U.S. hypersonics

After half a century of intermittent work on hypersonic vehicles, U.S. interest in developing BGVs grew following the September 11, 2001, terrorist attacks.¹⁹ They were seen as a way to deliver prompt, global attacks with conventional (non-nuclear) weapons against threats such as terrorist organizations and activities.²⁰ While ballistic missiles could be modified for this mission, U.S. long-range ballistic missiles are only used with nuclear warheads. Using BGVs would reduce the risk that the launch of a long-range strike might be construed as the beginning of a nuclear attack, prompting a

nuclear exchange. This interest led to the development of the HTV-2 vehicle as part of the Force Application and Launch from CONTinental United States (FALCON) program, announced in 2003 and run by the Defense Advanced Research Projects Agency (DARPA). The HTV-2 was intended to reach glide speeds greater than Mach 20 and a range of about 7,000 km.²¹

The HTV-2 vehicle was based in part on “waverider” designs proposed in the early 1950s.²² These designs use a wedge or half-cone shape intended to match the shock-wave pattern of the airflow around the glider, enclosing part of the shock wave under the vehicle to provide additional lift. Since the shock pattern depends on the vehicle’s speed and altitude, this concept could not be applied directly to long-range vehicles, since their speed and altitude can change significantly during the glide phase.²³ Drawing on this design, however, was used to improve vehicle performance by increasing its lift-to-drag ratio (L/D), which is a key parameter of BGVs. The HTV-2 demonstrated L/D of about 2.6 in tests.²⁴ (See [Appendix B](#) for the implications of increasing L/D .)

Around 2003 the Department of Defense (DoD) started a parallel track for developing a long-range BGV, called the Advanced Hypersonic Weapon (AHW).²⁵ It was based on a MaRV design—the Sandia Winged Energetic Reentry Vehicle Experiment (SWERVE)—that originated in the late 1970s and was flight tested through the mid-1980s.²⁶ Like the SWERVE, the AHW had a conical body with fins, rather than a wedge shape; DoD officials saw this design as a more technologically mature backup to the FALCON program.²⁷ The AHW had one successful test, in 2011, reaching 3,700 km with a speed of about Mach 7, although the goal was to reach 6,000 km and Mach 9–10.²⁸

By the mid-2010s, U.S. focus shifted to shorter-range hypersonic weapons with speeds of Mach 5–12 and ranges of a few thousand kilometers, in part due to difficulties with the HTV-2 tests.²⁹ In addition, the mission for hypersonic weapons changed: Use in theater-scale conflicts to evade or destroy defensive systems became a key motivation.

U.S. development then focused on two BGV designs. DARPA began developing a short-range wedge vehicle called the Tactical Boost Glide (TBG) system. DoD also began developing a short-range conical vehicle, called the Common Hyper Glide Body (C-HGB), based on the AHW.

In 2018, DoD’s goal was to produce the C-HGB for joint use by the Army, Navy, and Air Force, with each service using its own booster system. The Army’s program is the Long-Range Hypersonic Weapon (LRHW), and the Navy’s is the Conventional Prompt Strike (CPS) weapon.³⁰ The Air Force terminated its version of this program, the Hypersonic Conventional Strike Weapon (HCSW), in 2020.³¹

The LRHW and CPS reportedly have a total range greater than 2,775 km, roughly half of which is the glide phase.³² This range implies an initial speed of about Mach 10–12.

The conical C-HGB, as a descendent of the SWERVE and AHW, is clearly derived from MaRV designs. It has an estimated L/D of about 2.2—lower than the HTV-2's L/D of 2.6.³³ As a result, DoD's decision to pursue a conical design will likely result in a BGV with less range and maneuverability than a successful wedge design with higher L/D would have.³⁴ This also means that our estimates in Paper 1, based on the HTV-2, may somewhat over-estimate the flight performance of the C-HGB.

In 2019, the Air Force joined DARPA on the TBG program to develop an air-launched BGV—the Air-launched Rapid Response Weapon (ARRW)—intended to have a total range of about 1,600 km and average speed of Mach 6.5–8.³⁵ The Air Force reportedly saw ARRW as potentially lighter than the C-HGB, allowing an aircraft to carry more of them.³⁶ In early 2023, following multiple failed tests, it announced that it did not plan to procure ARRW vehicles but would finish development tests to provide data for future programs.³⁷

The United States and other countries have also been developing HCMs powered by air-breathing engines called scramjets, with speeds of Mach 5–10 and ranges of up to a couple thousand kilometers. From 2009 through 2013, the United States tested the X-51A HCM, which reached Mach 5.1; a DARPA/Air Force program to develop the Hypersonic Air-breathing Weapon Concept (HAWC) HCM builds on this program.³⁸

Scramjets for military HCM programs like the X-51 use hydrocarbon fuels rather than hydrogen fuel, which the earlier U.S. NASA X-43 vehicle used.³⁹ Using hydrocarbons limits their speed to below about Mach 8–10.⁴⁰ In 2020 Mark Lewis, then director of modernization at the DoD's Research and Engineering office, said he expects air-breathing systems will “probably top out around Mach 7,” which may limit their utility for certain missions, as discussed below.⁴¹

In addition to its long-range Avangard BGV, Russia has tested a ship-based HCM, the Tsirkon (Zircon), which is reported to reach Mach 6–8 and ranges of 400–1,000 km.⁴² Russia's Kinzhal (Dagger) weapon is an air-launched ballistic missile that maneuvers during reentry using fins, rather than a BGV. It reportedly reaches Mach 10, with a range up to about 1,500 km.⁴³

China's DF-ZF (previously called WU-14) is a BGV carried on a DF-17 booster, reportedly able to reach Mach 5–10 and a range of 1,200 km.⁴⁴ China declared it operational in October 2019.⁴⁵ China is also developing a wedge-shaped HCM called the Xingkong-2 (Starry Sky II). During its first test in August 2018, it reportedly reached Mach 5.5–6, traveling at 29–30 km

altitude for 400 seconds, which gives a glide range of 660–720 km.⁴⁶ Some reports suggest the vehicle could be operational in the mid-2020s.⁴⁷

As discussed, a key U.S. motivation for developing current BGVs is to evade terminal missile defenses. Whether a BGV (or HCM) can do so depends on its speed and design, as discussed below.

The capability of missile defenses against hypersonic weapons

This section assesses the ability of existing missile defenses to intercept hypersonic weapons and identifies the characteristics a weapon needs to evade interceptors.

The vulnerability of a vehicle to a specific defensive system depends in part on its flight altitude relative to the operational altitude window of the interceptor. A BGV's equilibrium glide altitude is determined by its speed, mass m , and lift coefficient C_L , or alternately by its speed, L/D , and ballistic coefficient $\beta = m/(C_D A)$, for drag coefficient C_D and reference area A . For $L/D = 2.6$ and $\beta = 7,500 \text{ kg/m}^2$, a BGV will glide at 28 km at Mach 5 and 38 km at Mach 10.⁴⁸

It is important to recognize that BGV dynamics during glide phase (velocity profile, range, and flight time) depend almost entirely on L/D and very weakly on β for a given initial glide speed V : Changing β will change the drag at a given altitude but also change the glide altitude so that the vehicle feels essentially the same drag force (see [Appendix B](#)).

Two types of missile defenses are currently deployed. Midcourse defenses, such as the U.S. Ground-based Midcourse Defense (GMD) and Aegis Standard Missile-3 (SM-3) systems, engage weapons at long distances and high altitudes when they are traveling on predictable trajectories above the atmosphere. Such “exo-atmospheric” defenses must operate at altitudes of 100 km or higher and in principle can defend large ground areas.

Terminal defenses engage weapons late in flight when they are reentering the atmosphere above their target. These defenses, including the U.S. Patriot and Aegis SM-6, and Russia's S-400 and S-500, maneuver aerodynamically and must operate at tens of kilometers altitude, meaning they are “endo-atmospheric.”⁴⁹ They engage weapons at short ranges and protect at most small ground areas. (The U.S. THAAD system operates in the high-endo to low-exo-atmospheric regions—see below.)

More information is available about U.S. defenses than those of other countries. We therefore model U.S. systems and assume they are representative of what other countries deploy now or may soon.

GMD and SM-3 interceptors

The United States deploys two long-range exo-atmospheric interceptors: the Ground-Based Interceptors (GBI) of the GMD system, and the SM-3

interceptors of the Aegis Sea-Based Midcourse system deployed on ships. Both are hit-to-kill systems, meaning that the kill vehicle carried by the interceptor attempts to destroy a target by physically colliding with it. Both interceptors cannot engage targets below about 100 km altitude, due to heating of the kill vehicle's IR sensor at lower altitudes.⁵⁰ As a result, neither could engage BGVs once those vehicles are in their glide phases. Moreover, when the weapons are in their ballistic phase, the interceptors would be vulnerable to decoys and other countermeasures designed to penetrate exo-atmospheric defenses.⁵¹

THAAD

The Terminal High Altitude Area Defense (THAAD) is a hit-to-kill system designed to engage ballistic missile reentry vehicles as they are beginning to reenter the atmosphere below about 150 km altitude. The THAAD interceptor's speed is about Mach 9 and atmospheric heating of its IR sensor restricts its use to altitudes above 40 km.⁵² The interceptor has two sets of thrusters for maneuvering: a set near the center to provide divert forces at high altitudes, and a set near the rear of the vehicle for attitude control, which allows maneuvering at lower altitudes by tipping the missile and creating atmospheric lift forces.⁵³

Since BGVs slower than about Mach 10 would glide at altitudes below about 40 km, THAAD could not engage them during their glide phase.

THAAD might be able to engage BGVs or MaRVs near the end of their ballistic phase as they reenter the upper atmosphere, where the atmospheric density might be too low for these weapons to generate sufficient lift forces to out-maneuver the interceptor. Since its operational range is only about 200 km, however, THAAD interceptors co-located with the weapon's target could not reach a BGV before the start of its glide phase; they might also not be able to reach a MaRV on a depressed trajectory before its altitude was too low. THAAD might be able to engage the weapon during its pre-glide phase if it was forward-deployed and positioned essentially under the weapon's trajectory, although the defense is not likely to know the location of the trajectory in advance if the BGV is fired from a mobile platform.

Moreover, at higher altitudes when the weapons are still in their ballistic phase, THAAD would be vulnerable to decoys and other countermeasures, as above. These countermeasures would not work at lower altitudes but could prevent THAAD from identifying the warhead and launching early enough to intercept above 40 km.

As a result, THAAD could not intercept BGVs in their glide phase and is not well-suited to engaging prior to the glide phase.

Patriot and other terminal interceptors

Current terminal interceptors use aerodynamic forces to maneuver to hit missile warheads late in their trajectories when they are below about 40 km altitude. By intercepting so late, they can defend only small ground areas—typically a region a few tens of kilometers in radius. They can therefore attempt to defend small targets like some military installations, but covering a large, populated region would require many interceptors, which would have to be interspersed within the region.

Current U.S. terminal systems include versions of the Patriot Advanced Capability-3 (PAC-3) defense, as well as the Navy's SM-2 and SM-6 interceptors.

During typical exo-atmospheric engagements, the only force acting on the interceptor's target is gravity, and the dynamics of the intercept depend on the relative speed of the interceptor and target—the closing speed—rather than the objects' individual speeds. For endo-atmospheric engagements, however, both interceptor and target can maneuver aerodynamically, and what matters is the relative lateral acceleration that the two objects can achieve at the altitude of the engagement as each attempts to outmaneuver the other. The interceptor must be able to closely match evasive movements of the target.

An important principle of guidance and control theory is that interceptors must be able to achieve two to three times the lateral acceleration of a maneuvering target to reliably intercept it.⁵⁴ The estimated miss distance for an engagement will depend on specifics of the interceptor sensor and guidance system, as well as what the defense knows about the target and the kind of maneuvers the target may execute. The target will have a good idea of what maneuvers it can execute that will be most stressing for the interceptor.⁵⁵

The lateral acceleration a of an object with mass m , lift coefficient C_L (laterally oriented), and velocity V at an altitude with atmospheric density ρ is given by:

$$a = \frac{C_L A \rho V^2}{2m} \quad (1)$$

where A is a characteristic area associated with the body.

The relative acceleration of a target and interceptor at the same location, and therefore the same ρ , is:

$$\frac{a_{target}}{a_{Int}} = \left(\frac{m_{Int}}{m_{target}} \right) \left(\frac{(C_L A)_{target}}{(C_L A)_{Int}} \right) \left(\frac{V_{target}}{V_{Int}} \right)^2 \quad (2)$$

Note that the most important variable is the velocity ratio at intercept, since it enters as a square.

Both the target and interceptor generate lift forces by creating an angle-of-attack between their body axis and velocity vector.⁵⁶ At higher altitudes where ρ and therefore the lift force is relatively low, the maximum lateral acceleration is set by constraints on how large an angle-of-attack the body can achieve; at lower altitudes the maximum lateral acceleration is limited by the body's ability to withstand the associated forces.⁵⁷ We assume the interceptor and target have similar structural constraints, and do not consider them explicitly.

Lateral acceleration of an interceptor and BGV

We apply Equation 2 to compare the maneuverability of a representative endo-atmospheric interceptor and a BGV. We estimate the characteristics of the PAC-3 Missile Segment Enhancement (MSE) interceptor, which was fielded in 2016 as an advanced version of the PAC-3 interceptor and is currently one of the most capable endo-atmospheric interceptors.⁵⁸ The original PAC-3 is now called PAC-3 Cost Reduction Initiative (CRI).

For the BGV, we consider a model system similar to the HTV-2 and about which aerodynamic parameters are known: the Common Aero Vehicle (CAV), for which lift and drag coefficients have been calculated in a report by Phillips.⁵⁹ While this is a useful model for analyzing hypersonic vehicles, the wedge-shaped CAV may not be representative of conical designs like the C-HGB, which might have lower L/D and thus less maneuverability.

PAC-3 MSE parameters. The PAC-3 MSE interceptor has a body diameter $d = 0.29$ m and length $l = 5.3$ m, giving a length-to-diameter ratio of about 18.⁶⁰

The hit-to-kill MSE interceptor has a “lethality enhancer:” a set of rods that shoot out from the body to give it a larger lethal diameter.⁶¹ This increases somewhat the miss distance that will still allow the interceptor to hit its target, but that increase is not large enough to change the dynamic analysis below.

The CRI is reported to have a mass of about 315 kg with 158 kg of propellant, which implies a mass after burnout of about 160 kg; we assume the same mass for the MSE.⁶²

Based on the reported increase in intercept range of the MSE over the CRI, we estimate the MSE speed is about 1.8 km/s (Mach 6), compared to 1.4 km/s (Mach 4.7) for CRI.⁶³ The MSE is said to intercept at altitudes of 30+ km, compared to 20+ km for CRI.⁶⁴ It has a two-pulse motor; the second pulse might be used to maintain the interceptor's speed during flight (we assume the interceptor travels at its maximum speed throughout its flight).

At zero angle-of-attack (φ) the cylindrical MSE body will generate zero lift. To maneuver, a set of small thrusters around the body give it a non-zero φ , which creates lift. We estimate the lift coefficients for φ of 10–20° for the interceptor and BGV.

We estimate the lift coefficient of MSE from the normal force coefficient C_N of a cylindrical body:⁶⁵

$$C_N = \frac{A_b}{A} \sin 2\varphi \cos \frac{\varphi}{2} + \eta c_{dn} \frac{A_p}{A} \sin^2 \varphi \quad (3)$$

where A_b is the base area, A_p is the planform area, and A is referred to as a reference area of the body. For high Mach number, the parameters $c_{dn} \sim 1.3$ and $\eta \sim 1$, and are related to the crossflow drag of a cylinder.⁶⁶ For small φ , C_L is essentially equal to C_N .⁶⁷

The quantity appearing in Equations 1 and 2 is $C_L A$, which Equation 3 gives in terms of the known areas A_b and A_p . Using $A_p = ld$ and $A_b = \pi d^2/4$, Equation 3 at high Mach number becomes:

$$C_L A \approx C_N A = A_b \left[\sin 2\varphi \cos \frac{\varphi}{2} + \frac{5.2}{\pi} \frac{l}{d} \sin^2 \varphi \right] \quad (4)$$

Applying Equation 4 to the MSE with $l/d = 18$ gives the values in Table 1.

BGV parameters. To estimate the variation of the BGV's lift coefficient with φ , we use data for the CAV. We assume $L/D = 2.6$ and $m = 900$ kg, which are appropriate to the HTV-2.⁶⁸

Phillips' analysis presents aerodynamic parameters for two CAV models with different values of L/D , called the CAV-H and CAV-L, for “high” and “low” performance respectively.⁶⁹ The CAV-H model has a mass of 910 kg, a length of 2.7–3.7 m, and a diameter of 1.2 m, which is similar in size to the HTV-2.⁷⁰ While it has a somewhat higher L/D than the HTV-2 (3.0–3.3 at Mach 20 for φ in the range of 10–15°) we use its variation in lift values as a function of φ to estimate the approximate performance of related wedge-shaped gliders.⁷¹ The L/D of the CAV-H model is maximized near $\varphi = 10^\circ$ for speeds above about Mach 6.

We estimate the glider's lift using the values Phillips calculates for the CAV-H at Mach 6, which leads to the values in Table 2.

Table 1. Estimated lift values for the MSE interceptor at varying angle-of-attack.

φ	10°	15°	20°
$C_L A$	0.079	0.17	0.27

Implications for interception

Using Equation 2 and the requirement that the interceptor must generate two to three times the lateral acceleration of the target to reliably intercept it, we find the following requirement for the interceptor velocity V_{int} :

$$V_{int} \geq \left[(2 \text{ to } 3) \left(\frac{m_{Int}}{m_{target}} \right) \left(\frac{(C_{LA})_{target}}{(C_{LA})_{Int}} \right) \right]^{\frac{1}{2}} V_{target} \equiv \gamma V_{target} \quad (5)$$

where γ is defined as the expression multiplying V_{target} . Inserting the estimates of the MSE (interceptor) and CAV-H (target) parameters for ϕ in the range of 10–20° gives γ in the range 0.8–1.2. This leads to an approximate condition for the interceptor to be able to reliably intercept the target:

$$V_{int} \gtrsim V_{target} \quad (6)$$

This condition implies that an MSE interceptor cannot be expected to reliably intercept BGVs like the CAV traveling at speeds much greater than its own, and therefore could not reliably intercept a BGV traveling faster than about Mach 6 during the BGV's dive toward the ground.

The condition in Equation 6 will not depend strongly on details of the vehicles such as their mass and lift coefficient, because those parameters appear within a square root. This suggests that the key issue in developing a more capable interceptor is to increase its speed.

Note that the speeds typically cited for BGVs are their initial glide speeds, which will be significantly higher than their speeds during their dives because of drag. It is the speed at the engagement altitude, near the end of BGV flight, which is relevant in Equation 6.

Figure 1 shows the speed of a BGV with aerodynamic parameters similar to the HTV-2 during its dive, based on calculations described in Paper 1. The curves start at the glide altitude of the vehicle for velocities of Mach 5–10; the vehicle then dives by using lift forces to pull it downward.

The boxes in the lower left of Figure 1 show the approximate regions where interceptors like the PAC-3 CRI and MSE would likely be able to intercept the BGV during its dive, based on this analysis. At very low altitudes, defenses could not intercept BGVs even if they were traveling sufficiently slowly.

These results suggest that a BGV like the HTV-2 traveling faster than about Mach 10 at the start of its dive should have a speed above Mach 6

Table 2. Estimated lift values at Mach 6 for Phillips' model of the CAV-H using a reference area $a = 750 \text{ in}^2 = 0.48 \text{ m}^2$.

ϕ	10°	15°	20°
C_{LA}	0.20	0.33	0.47

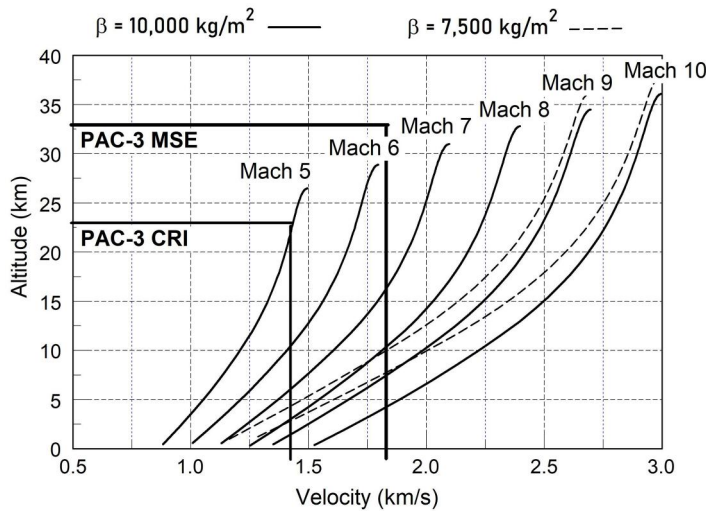


Figure 1. BGV speed during its dive from its glide altitude. Curves are labeled by the vehicle's speed at the start of its dive (i.e., at the end of glide). Solid curves assume $\beta = 10,000 \text{ kg/m}^2$ during the dive, and dashed curves assume $\beta = 7,500 \text{ kg/m}^2$; both assume $L/D = 2.6$. The boxes in the lower left show the regions where the PAC-3 CRI and MSE would likely be able to intercept such a vehicle during its dive. Interceptors may not be able to engage BGVs at very low altitudes.

throughout much of its dive, and thus be able to evade an interceptor like the MSE. If a key role of BGVs is to evade or attack terminal defenses, the attacker should fly these weapons in ways that ensures they have high enough speed (about Mach 10) at the end of their glide phase.

As an example, for a glide range of 1,000 km, a BGV like that considered here would need to begin its glide at about Mach 13 since it would slow to approximately Mach 10 during glide. Achieving high initial speed drives up the mass of the required booster. Alternately, a lower initial speed would limit the distance that a BGV could glide and still start its dive at Mach 10.

The solid curves in Figure 1 assume $\beta = 10,000 \text{ kg/m}^2$ for the BGV during its dive phase and the dashed curves assume $\beta = 7,500 \text{ kg/m}^2$. A recent study reports $\beta = 4,680 \text{ kg/m}^2$ for the HTV-2 vehicle at maximum L/D during glide, although it could be higher if the vehicle was flying with a lower value of L/D during the dive.⁷² For smaller values of β , the BGV will slow more during the dive, requiring it to start its dive with a speed greater than Mach 10 to evade defenses.

Current Aegis SM-2 and SM-6 interceptors have speeds of about Mach 4 and are therefore less effective against BGVs than are Patriot systems. While they use fragmentation warheads rather than hit-to-kill, they must still achieve small miss distances. The planned SM-6 Block IB will reportedly be faster than Mach 5, giving it somewhat greater capability, but still less than MSE.⁷³

Note that the engines on HCMs could counteract the speed loss due to drag during the glide phase, but the very high thrust needed to overcome drag due to the exponential increase in atmospheric density encountered during a dive would require an impractically large engine and fuel mass. As a result, even HCMs would require a high speed at the beginning of their dive to be able to evade defenses.

Defense against BGVs

As discussed, the current type of missile defense relevant to stopping attacks by BGVs of the ranges considered here is terminal defense.

Our analysis implies that defenses similar to PAC-3 MSE should be able to engage BGVs that have glide speeds at the start of dive of up to roughly Mach 10 and may therefore be able to defend small regions against these vehicles.

However, current ship-based interceptors like SM-2 and SM-6 may be too slow to effectively intercept such vehicles.

A key step for improving terminal defense capability is to increase the interceptor speed. The development of the MSE and the new SM-6, however, suggests that significant increases may be difficult to achieve. The United States is developing a new system—the Glide Phase Interceptor (GPI)—intended to engage during the BGV's glide phase. Doing so could allow longer-range intercepts, increasing the defended area, but GPI would need to be considerably faster than current interceptors since it would engage BGVs before they slowed during their dives, which raises similar heating issues.

To counter new defenses, the offense can attempt to develop faster BGVs. These vehicles would experience significantly higher heating rates and require more massive boosters.

Terminal defenses should be able to use ground-based radars to track and engage BGVs, since BGVs of the ranges considered here would typically glide at 30–40 km altitude, and radars could detect such vehicles at a range of about 400 km or longer. These radars could be cued by missile detection and tracking systems, such as the U.S. Space-Based IR System (SBIRS).⁷⁴

Appendix C contains a discussion of the role of new space-based sensors.

Comparing range, mass, and flight time of BGVs and MaRVs

As seen above, in analyzing hypersonic weapons one must consider not only their top speed, but their speeds throughout glide and dive phases.

We consider here how a BGV's speed is related to its mass, range, and delivery time, and how it changes during flight.

Increasing the maximum speed of a BGV or MaRV—the speed at the end of the boost phase—will increase its maximum range and decrease its flight time for a given range but will increase the mass of the booster needed to accelerate it to that speed. This mass increase can be significant since the rocket equation requires that booster mass grows exponentially with its burnout speed:⁷⁵

$$M_i = M_f e^{\Delta V/V_{ex}} \quad (7)$$

where M_i and M_f are the initial and final masses of the booster plus vehicle before and after burning fuel to bring about a velocity increase of ΔV . V_{ex} is the booster's exhaust velocity.

We refer to the mass of the BGV and MaRV vehicles as the “vehicle mass” and the mass of the vehicle + booster as the “total mass” of the weapon. Equation 7 shows that the total mass depends on the vehicle mass and the speed to which the booster accelerates it. Total mass is an important issue for air-launched systems since it limits the number of weapons an aircraft can carry.

For context, current U.S. air-launched missiles appear to have masses of between 1,000 and 2,000 kg.⁷⁶ The DoD has reported the mass of the ARRW plus booster as about 2,300 kg.⁷⁷ The payload capability of a B52-H bomber is reported to be 32,000 kg; the B1-B heavy bomber is reported to be able to carry about twice that amount, including munitions carried internally and on external mounts.⁷⁸

The Army and Navy are likely less concerned about large mass for systems launched from land or surface ships, although large systems can raise challenges, for example in submarines.

Below we estimate the relative ranges, booster masses, and flight times for BGVs and MaRVs focusing on two scenarios, in which:

1. The vehicles have a speed of Mach 5 when they begin their dive to their targets. We refer to this as the Mach 5 scenario. As shown above, these vehicles may be vulnerable to interception by terminal defenses.
2. The vehicles maintain higher speeds during their dive phase to allow them to evade terminal defenses. As discussed above, that currently appears to require a BGV or MaRV keep its speed above about Mach 6 to low altitudes, which requires a BGV to have a speed above about Mach 10 when it starts its dive. To be conservative, the analysis below assumes a speed of Mach 9 at the start of dive. We refer to this as the Mach 9 scenario.

In this section we ignore BGV maneuvering during its glide phase, which will reduce its speed and range. We return to that issue below.

To allow comparison, we first assume the BGV and MaRV vehicles have the same mass and aerodynamic parameters. This means the MaRV is essentially the BGV vehicle fired on a predominantly ballistic rather than a gliding trajectory; it would have a similar ability to maneuver during reentry but would not use lift prior to that. We assume both vehicles have masses of 700 kg, which is somewhat less than the 900–1,000 kg reported for the HTV-2 vehicle.⁷⁹

In reality, since the MaRV vehicle does not experience the long period of atmospheric stress and heating that the BGV does during its glide phase, the MaRV could likely be lighter than a BGV of the same range, leading to a proportionate decrease in booster mass.

For example, in the 2000s the United States flight tested a MaRV being developed for the Conventional Trident Modification (CTM); it was based on the Mk-4 reentry vehicle with flaps for aerodynamic maneuvering to give high accuracy.⁸⁰ The CTM's intended range was more than 6,000 km, with a considerably higher reentry speed (near Mach 20) than the systems considered below, yet its reported mass was only 120 kg.⁸¹ While increasing the maneuverability of this system would require additional heat shielding, its low mass suggests a more capable MaRV could still have a mass well below 700 kg, especially if it was intended for ranges of a few thousand kilometers.

We therefore also consider below how the results would change if the MaRV were less massive than the BGV.

Estimating booster mass

With these assumptions, we estimate the total mass and the standoff range at which each system can be launched.

We first consider air-launched BGVs and MaRVs, since air-launching is a scenario in which booster mass could be critical. We assume the aircraft is flying at 10 km altitude at booster launch and that the booster burns out at an altitude of 40 km, with varying burnout speeds and velocity angles; changing the launch and burnout altitudes has little effect on the results.

To estimate the mass of the required booster, we use an equation derived from Equation 7 assuming the booster has n stages and accelerates the vehicle to a speed V . Each stage has a fuel fraction f (equal to the propellant mass of the stage divided by the total stage mass) and an exhaust velocity V_{ex} and the booster experiences gravity and drag losses of δV :⁸²

$$\frac{M_{tot}}{m} = \left\{ 1 - \left[1 - \exp\left(-\frac{V + \delta V}{nV_{ex}}\right) \right] / f \right\}^{-n} \quad (8)$$

Here m is the mass of the payload—the BGV or MaRV vehicle. M_{tot} is the total mass of the booster plus vehicle. For a solid booster of this size, we assume $V_{ex} = 2.8$ km/s and $f = 0.87$, which includes the mass of the interstage sections. Assuming the booster is launched at 10 km and burns out at 40 km altitude, δV is about 0.3 km/s.

Our calculations assume $n = 2$ stages. While two stages may not be needed or desirable at the lower end of the hypersonic regime, Equation 8 gives similar values for low speeds using $n = 1$ or 2. The total mass increases roughly exponentially with booster speed.

MaRV range and flight time estimates

For a given speed and velocity angle at booster burnout, we calculate the MaRV range and flight time numerically using the trajectory model in Paper 1, assuming a standard atmosphere and a ballistic coefficient of $\beta = 7,500\text{--}10,000$ kg/m².⁸³ As noted, we assume burnout occurs at 40 km altitude. The vehicle uses lift forces during reentry to dive more steeply, just as BGVs do; this allows a faster descent and less slowing due to drag. We assume L/D of -1 to -2 when the MaRV is below 30 km altitude (where the minus sign means the lift force is pulling downward), with the value chosen to give a nearly vertical impact at the ground. Varying the altitude at which the dive begins or the value of L/D has little effect on the total calculated range and flight time.

We consider missile ranges up to 3,000 km, with three cases for each range, in which the MaRV is launched (1) on an MET (with a burnout angle near 40°), (2) on a DT with a burnout angle of 30°, and (3) on a DT with a burnout angle of 20°. For each range, these burnout angles determine the required burnout speed and therefore the total mass of the weapon.

The total ranges and flight times we calculate are the distances and times after booster burnout (i.e., from the start of the ballistic phase); including the booster's powered phase would add approximately 100–150 km of range and 1.5 minutes of flight time but would depend on the details of the booster and flyout trajectory.

BGV range and flight time estimates

BGV flight consists of several stages: a ballistic phase, a pull-up phase as it reenters the atmosphere and maneuvers onto a horizontal glide trajectory at the appropriate altitude, a glide phase, and the final dive phase. Note that in discussions of BGVs, “range” may be used to refer to glide range vs. total range; we attempt to be explicit about this in the discussion below.

As above, we calculate the range and time of the ballistic phase numerically given a speed (V_{bo}) and angle (γ_{bo}) at burnout, which is assumed to take place at 40 km altitude. The ballistic phase ends at an altitude h_0 a few kilometers above the initial glide altitude, which is set by the vehicle's speed at the beginning of glide and its values of L/D and β (see below). The speed and angle at the end of the ballistic phase are V_0 and $-\gamma_0$, respectively (the minus sign makes γ_0 a positive number).

The range and flight time of the dive phase are calculated numerically, starting with the vehicle's speed and altitude at the end of glide phase, and assuming L/D of -1 to -2 , as above. Our calculations assume $\beta = 7,500 \text{ kg/m}^2$ for the BGV.⁸⁴

If a BGV's value of β were lower than this, its dive time would increase somewhat because the dive would begin at a higher glide altitude and the BGV would slow more during the dive. More importantly, because it would increase drag during the dive, a lower value of β would require the BGV to start its dive with a speed greater than Mach 9 in order to evade defenses during dive. Requiring a higher speed would increase the total mass of the BGV above those calculated below.

Equations for the pull-up phase. To maneuver into its glide phase, the BGV undergoes a "pull-up" maneuver that takes it from reentering at an angle $-\gamma_0$ to gliding at its equilibrium altitude with $\gamma \sim 0$. This maneuver reduces the vehicle's speed before it begins its glide, and this reduction can have an important effect on BGV range.

We use Acton's equations for the pull-up phase, which we put in the form of [Equations 9–12](#) for the change in speed (V), altitude (h), time (t), and range (r), where the subscripts 0 and 1 refer to the start and end of pull-up, respectively, and the vehicle maneuvers from a reentry angle of $-\gamma_0$ to 0:⁸⁵

$$\frac{V_0 - V_1}{V_0} = \frac{\gamma_0}{\frac{L}{D}\Delta} \quad (9)$$

$$h_0 - h_1 = \frac{\gamma_0^2 R_{turn}}{2\Delta} \quad (10)$$

$$t_1 - t_0 = \frac{\gamma_0 R_{turn}}{V_0 \Delta} \quad (11)$$

$$r_1 - r_0 = \frac{\gamma_0 R_{turn}}{\Delta} \left(1 - \frac{\gamma_0}{2 \frac{L}{D} \Delta} \right) \quad (12)$$

where

$$\Delta \equiv 1 - \frac{\alpha_0 g R_{turn}}{V_0^2} \quad (13)$$

$$\alpha_0 \equiv \alpha(V_0) = 1 - \frac{V_0^2}{V_e^2} \quad (14)$$

and $V_e = [g(R_e + h)]^{0.5} \sim 8 \text{ km/s}$ for the altitudes of interest here, where R_e is the Earth radius.

The constant R_{turn} has units of length and is essentially the turning radius of the pull-up maneuver. Acton relates it to parameters of the vehicle as:

$$R_{turn} = \frac{2\beta}{L/D\rho_1} = \frac{1}{\alpha_1} \left(\frac{V_1}{V_e} \right)^2 (R_e + h_1) \quad (15)$$

where ρ_1 is the atmospheric density at the end of the pull-up phase, and the second equality uses Equation 14, and Equation 19 for ρ_1 ; h_1 is the initial glide altitude. Alternatively, as discussed below, R_{turn} can be considered a parameter chosen to optimize the pull-up maneuver.

Note that the second term on the right-hand side of Equation 13 can be written as:

$$\frac{\alpha_0 g}{V_0^2 / R_{turn}} \quad (16)$$

which is the ratio of the effective gravitational acceleration (g reduced by the inertial factor α_0) to the centripetal acceleration of the vehicle due to its pull-up maneuver. For high speeds or sharp turns, this term is small so that $\Delta \sim 1$ and Equations 6–9 reduce to the simple form in which the velocity change depends only on γ_0 and L/D , and not R_{turn} .⁸⁶ We use the full equations for our calculations.

Figure 2 shows how the speed change during pull-up, $\delta V = V_0 - V_1$ given by Equation 9, varies with R_{turn} for the case of $\gamma_0 = 5^\circ$, $L/D = 2.6$, and several values of V_0 . As discussed, for large V_0 , δV varies slowly with R_{turn} . To reduce speed loss during pull-up the vehicle should turn using a small value of R_{turn} . Too small a value of R_{turn} will lead to high stresses; keeping the associated forces below 15g, which appears to be a conservative value based on modern airframes, gives minimum values of R_{turn} of 42 km for $V_0 = 2.5 \text{ km/s}$ to 135 km for 4.5 km/s.⁸⁷

Equation 10 shows that the choice of R_{turn} will determine the altitude change during pull-up, which is the difference in altitude between the end of the ballistic phase and the beginning of equilibrium glide. Calculations show that the overall range and flight time results for the BGV are insensitive to the particular choice of R_{turn} as long as it is in the region of the curve in which δV does not vary rapidly. Figure 3 shows the values of R_{turn} we use for a given velocity and angle at the start of pull-up.

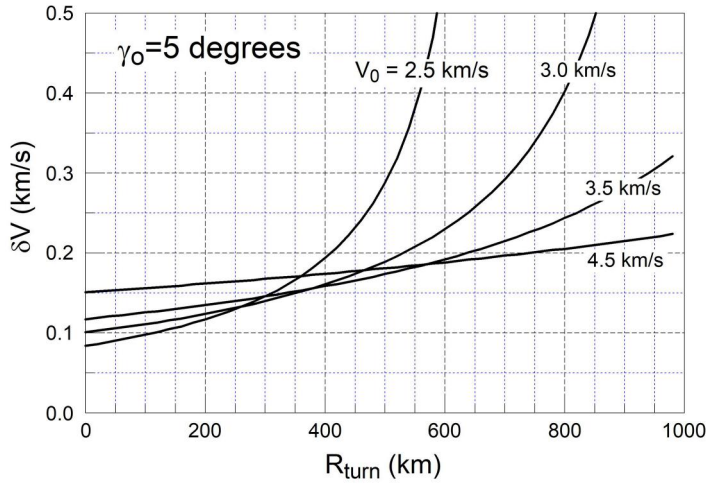


Figure 2. Speed change during pull-up, $\delta V = V_0 - V_I$, as a function of R_{turn} for $\gamma_0 = 5^\circ$ and $L/D = 2.6$.

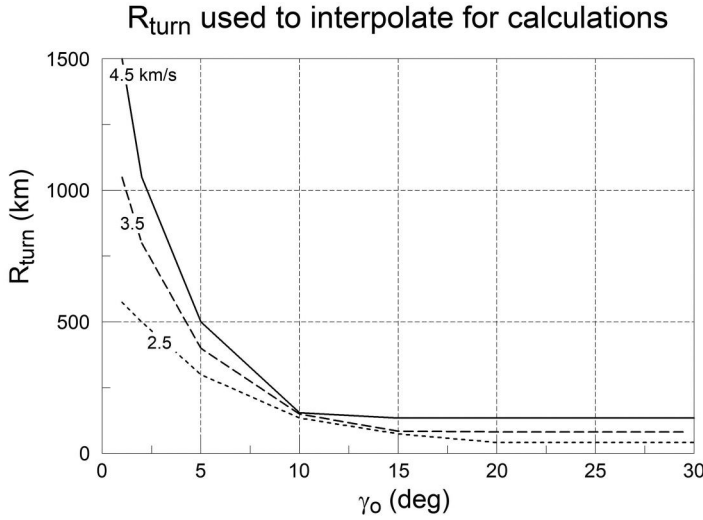


Figure 3. The curves used to interpolate the value of R_{turn} for a given velocity and angle γ_0 at the start of pull-up, chosen to give low values of δV and appropriate values of altitude change for the associated speed and $\delta\gamma$.

Equations for the glide phase. The drag force on the vehicle during glide is:

$$F_D = \frac{1}{2} C_D A \rho V^2 = \frac{\rho}{2\beta} m V^2 \quad (17)$$

The equations of motion show the lift force must equal the vehicle weight mg reduced by an inertial term due to its flight over a spherical Earth:

$$F_L = \left(1 - \frac{V^2}{V_e^2} \right) mg \equiv \alpha mg \quad (18)$$

where $\alpha(V)$ is given by Equation 14 and includes the inertial (centrifugal) effects at high speed. Since $F_L = (L/D)F_D$, combining Equations 17 and 18 gives the equilibrium glide altitude h of the vehicle at speed V , where h corresponds to the atmospheric density satisfying:

$$\rho(h) = \frac{2\alpha g \beta}{L/D V^2} \quad (19)$$

F_D can then be written:

$$F_D = m \frac{\alpha g}{L/D} \quad (20)$$

Equation 20 shows that although F_D appears from Equation 17 to vary as V^2 , as V changes during glide the vehicle will change its glide altitude to produce a lift force given by Equation 18, which removes most of the velocity dependence of F_D . Because of this, F_D has only a weak velocity dependence through α , which varies by less than 10% as V changes from Mach 5 to Mach 10.

We use Equation 20 to derive expressions for BGV glide dynamics. Ignoring the very small change in potential energy of the BGV as its altitude changes during glide, the BGV's change in kinetic energy during glide equals the work done by drag:

$$d\left(\frac{mV^2}{2}\right) = -F_D dr = -\frac{mg}{L/D} \left(1 - \frac{V^2}{V_e^2}\right) dr \quad (21)$$

Appendix D shows this can be integrated and put in the form (where $\alpha_g = \alpha(V_g)$):

$$V(r_G) = V_e \left[1 - \alpha_g \exp\left(\frac{2gr_G}{L/D V_e^2}\right) \right]^{1/2} \quad (22)$$

which gives the speed for a BGV that starts gliding with a speed V_g and glides a distance r_G .

Equation 22 gives the glide range of a BGV starting at V_g and ending at V_f as:

$$r_G(V_g, V_f) = \frac{L/D V_e^2}{2g} \ln \left(\frac{1 - V_f^2/V_e^2}{1 - V_g^2/V_e^2} \right) \quad (23)$$

Appendix D shows that Equation 22 can also be used to derive the time duration of glide over distance r_G :

$$t_G(r_G) = \frac{r_G}{V_e} - \frac{L/D V_e}{g} \ln \left[\frac{1 + \left(1 - \alpha_g \exp\left(\frac{2gr_G}{L/D V_e^2}\right)\right)^{1/2}}{1 + V_g/V_e} \right] \quad (24)$$

Equations 23 and 24 can be used to derive an equation for the time duration of glide starting at V_g and ending at V_f :

$$t_G(V_1, V_f) = \frac{L/D V_e}{2g} \ln \left[\frac{(1 - V_f/V_e)(1 + V_g/V_e)}{(1 + V_f/V_e)(1 - V_g/V_e)} \right] \quad (25)$$

Notice that these equations depend on L/D but not β .

These equations allow us to estimate the BGV range and flight time for a given booster burnout speed V_{bo} and angle γ_{bo} (determined by the boost phase trajectory). Given those burnout values, we calculate the range, speed, and angle at the end of the ballistic phase, and use those numbers to calculate the range and speed at the end of the pull-up phase, at which point the BGV is on a glide trajectory with $\gamma=0$. The BGV then glides until it slows to V_f and then dives to the ground. The total range is the sum of the ranges during the ballistic, pull-up, glide, and dive phases.

To calculate the curves in the plots below we choose values of V_{bo} and γ_{bo} such that the glide range is roughly half the total range in each case, although the results are not sensitive to this choice.⁸⁸

To do this, for a total range R and speed V_f at the end of glide (where $V_f = \text{Mach } 5$ or $\text{Mach } 9$) we vary V_{bo} and γ_{bo} to find a combination with the smallest V_{bo} (and therefore the smallest total mass of the weapon for a given vehicle mass) that gives a total range R and glide range $r_G = R/2$, subject to the constraint that the BGV dives from its glide phase when it reaches a speed V_f . For each range R and speed V_f that allows us to calculate the flight time and a total vehicle mass (from Equation 8).

The speeds, angles, ranges, and flight time for the ballistic and terminal phases of the BGVs and MaRVs are determined by numerical calculations of the trajectory using the model described in Paper 1.

In particular, our calculations follow these steps:

1. Assume the ballistic phase begins with booster burnout at 40 km altitude, with speed V_{bo} and angle γ_{bo} . Calculate the range, time, speed, and angle at the end of the ballistic phase (which is the beginning of the pull-up phase). This will typically occur a few kilometers above the altitude at which glide will begin (for most of our calculations we assume the pull-up phase begins at about 40 km).

2. Pick an appropriate value of R_{turn} for the speed and angle at the beginning of pull-up and use Equations 9–14 to calculate the speed, range, altitude, and time at the end of the pull-up phase.
3. Assume the vehicle starts glide with $\gamma=0$ and its speed at the end of pull-up, at an altitude given by Equation 19.
4. Calculate the glide range and time using Equations 23 and 25 assuming glide ends when the BGV reaches V_f .
5. Calculate the range and time of the dive phase given the vehicle's speed and altitude at the end of glide phase.
6. Sum the range and flight time for the ballistic, pull-up, glide, and dive phases.
7. Iterate this process varying V_{bo} and γ_{bo} to find values that give a trajectory for which the glide range is roughly half of the total range.
8. Calculate the total mass of the weapon for this value of V_{bo} using Equation 8.

Comparing BGVs and MaRVs for short ranges

In this section, we compare the ranges, flight times, and masses of BGVs and MaRVs for total ranges up to about 1,200 km. Since these weapons may be air-launched, the total mass is an important consideration. The systems considered in this section have total masses of 2,000–4,000 kg.

As noted, the BGV is assumed to have $L/D=2.6$, which is the value estimated for the HTV-2; the MaRV is assumed to have $L/D=0$ until it reaches 30 km altitude on reentry, below which it has L/D of -1 to -2 .⁸⁹ The results for the two systems will be approximate, both because the analysis is approximate and the parameter values are uncertain. But our primary interest is estimating the *relative* capability of the two systems, which should be fairly insensitive to these details.

Figure 4 shows the total mass as a function of range, assuming both vehicles have a mass of 700 kg. In this case, equal total mass means the vehicles have the same burnout speed.

If the vehicle masses are larger or smaller than 700 kg, then the curves in Figure 4 will move up or down by the ratio of the actual vehicle mass to 700 kg.

Figure 5 shows the results if the MaRV mass can be reduced relative to the BGV, because of reduced heat shielding or structural requirements as discussed above. In that case, Equation 8 shows that the total mass of the MaRV plus booster could be reduced compared to the BGV by a similar fraction as the reduction of vehicle mass, while maintaining the same burnout velocity. Figure 5 compares the total masses assuming the BGV vehicle has a mass of 700 kg and the MaRV vehicle has a mass of either 500 or 350 kg.

Figure 6 shows the flight time of the vehicles in Figures 4 and 5 as a function of range. The lines correspond to the smallest total mass for each range and vehicle mass, as shown in Figures 4 and 5.

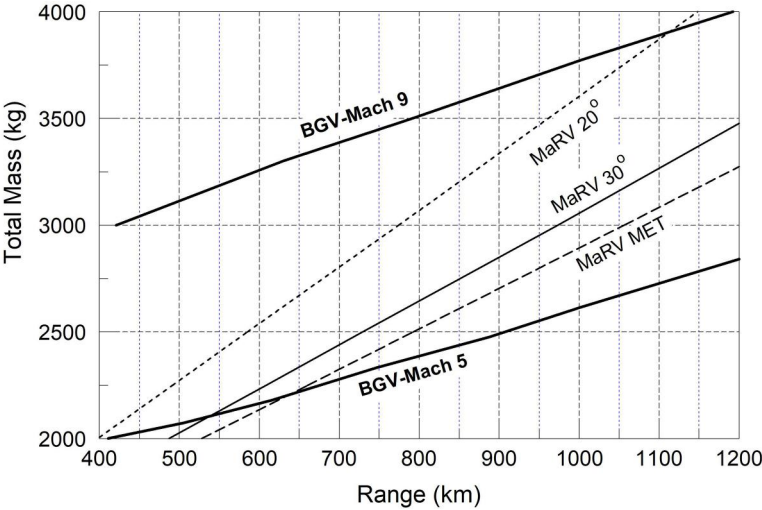


Figure 4. Smallest total mass required to reach a given range assuming BGV and MaRV vehicle masses are 700 kg, for a MaRV (thin lines) on an MET (burnout angle about 40°) and on DTs with burnout angles of 20° and 30° , and a BGV (bold lines) on a trajectory for which the glide range is half the total range. Speed at the end of BGV glide phase is either Mach 5 or Mach 9. Range is the sum of the ranges during ballistic, pull-up, glide, and dive phases.

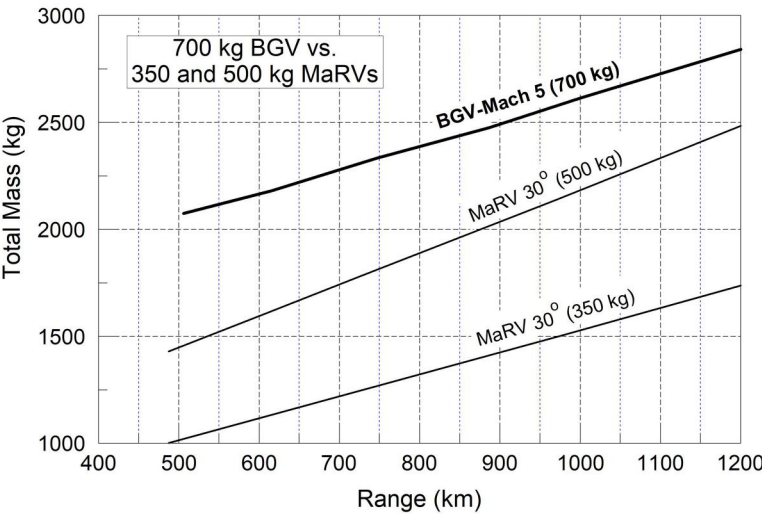


Figure 5. The results shown in Figure 4 for the Mach 5 BGV and 30° MaRV, but in which 350- and 500-kg MaRVs are compared to the 700-kg BGV shown in that Figure. The burnout speed of the MaRVs for each range is the same as in Figure 4 so their total mass is reduced by the ratio of the MaRV vehicles assumed in the two cases (350/700 and 500/700).

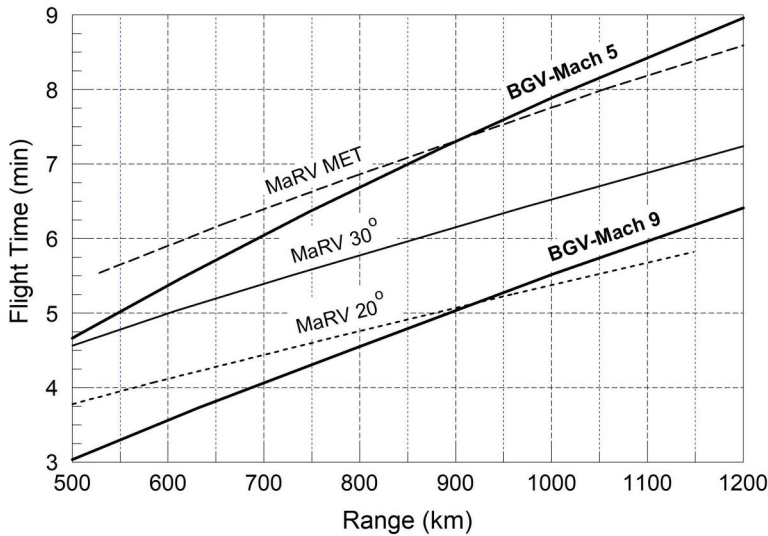


Figure 6. Flight time versus range for the scenarios described in Figures 4 and 5. The lines correspond to the smallest total mass for each range and vehicle mass, as shown in Figures 4 and 5.

Implications for short ranges

For clarity we refer to BGVs with speeds of Mach 5 and Mach 9 at the end of their glide phase as BGV-5 and BGV-9, respectively.

Mach 9 case. Under the assumptions in our analysis, a key implication is that if aircraft only carry weapons with masses less than about 3,000 kg they will not be able to carry a BGV-9 with a range of more than about 400 km (Figure 4) unless the BGV vehicle mass is less than 700 kg. In contrast, a 700-kg MaRV vehicle with a total mass of about 3,000 kg could be launched from a range of about 1,000 km while maintaining speed sufficient to evade defenses. Lower mass MaRV vehicles could be launched from much greater distances (Figure 5).

Mach 5 case. Aircraft could launch BGV-5s with total mass below 3,000 kg from ranges of about 1,300 km. A BGV-5 will typically have a longer range than a MaRV with the same total mass, assuming equal vehicle masses (Figure 4).

For low total masses (around 2,500 kg) this range difference is relatively small: A 2,500 kg air-launched BGV-5 could have a range up to about 900 km compared to about 800 km for a MaRV of the same mass launched on an MET—a difference of about 10%—and the two vehicles would have similar flight times.

For a 3,000 kg weapon, the BGV-5 could have a range of about 1,300 km compared to 1,050 km for a 700-kg MaRV on an MET or 970 km on a 30° trajectory—a difference of 20–25%. The range advantage of the BGV-5

increases with larger total mass, as discussed below, but such weapons are unlikely to be air-launched.

If, however, MaRV vehicle mass can be reduced relative to the BGV-5 then the range advantage of the BGV-5 disappears. Figure 5 shows that a 500 kg MaRV vehicle can reach 1,200 km on a 30° trajectory with a 2,500 kg total mass, compared to 900 km for a BGV-5 with the same total mass and a 700 kg vehicle mass. A BGV-5 with a 2,800 kg total mass could also reach a range of 1,200 km, but its flight time would be longer than the MaRV by more than a minute and a half.

Figure 5 shows that the MaRV's range advantage will increase significantly if its mass can be made even lighter.

Comparing BGVs and MaRVs for longer ranges

We next compare BGV and MaRV for total ranges up to 3,000 km.

For ranges much longer than 1,000 km, 700-kg BGV and MaRV vehicles with their boosters would be massive enough that they would likely be launched from ships or land rather than aircraft. One of the few estimates available of the total mass of the Army's ground-launched LRHW, with a reported total range of about 3,000 km, is more than 7,000 kg.⁹⁰

As above, we consider the two cases in which the BGV speed is either Mach 5 or Mach 9 when it starts its dive to the target. We again assume that the glide range is half of the total range and assume that burnout occurs at about 50 km for surface launches; the results are not sensitive to this assumption.

Figure 7 shows the total mass of the weapon as a function of its range, assuming both BGV and MaRV vehicle masses are 700 kg; in this case, equal total mass means the vehicles have the same burnout speed. As above, this plot shows the relative capabilities of the two systems; if the vehicle masses are larger or smaller than 700 kg, then the curves in Figure 7 will move up or down by the ratio of the actual vehicle mass to 700 kg.

Figure 8 shows how Figure 7 changes if the MaRV mass can be reduced relative to the BGV. It compares the 700-kg BGV in Figure 7 with a 500-kg and 350-kg MaRV flown on a 30° trajectory with the same burnout speed as in Figure 7. Equation 8 shows that the total mass will decrease by the ratio of the vehicle masses, with the same performance.

Figure 9 shows the flight time of the vehicles in Figures 7 and 8 as a function of range. The points correspond to the smallest total mass for each range and vehicle mass, as shown in Figures 7 and 8.

Figures 7 and 9 show that, for a given range, decreasing the burnout angle of a MaRV from its MET value (near 40°) to 30° leads to only a small increase in the required booster speed, and therefore mass, but significantly reduces the flight time.

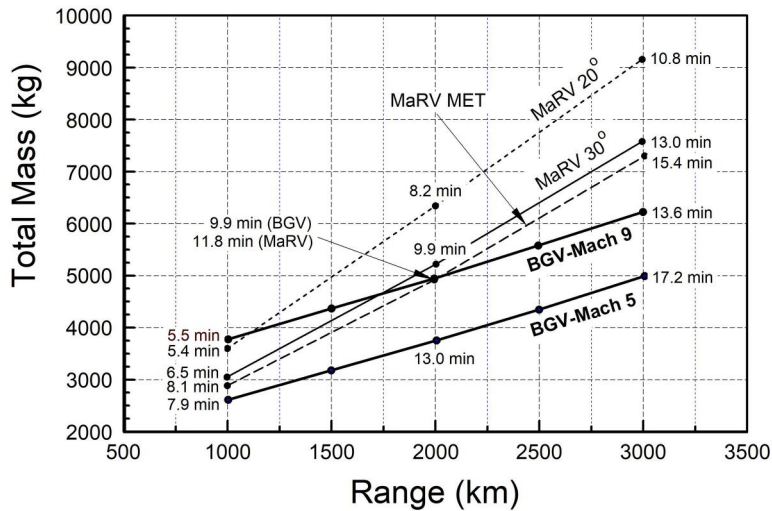


Figure 7. Minimum total mass required to reach a given range assuming the BGV and MaRV vehicle masses are 700 kg, for a MaRV (thin lines) on an MET (burnout angle about 40°) and DTs with burnout angles of 20° and 30° , and a BGV (bold lines) with a burnout velocity that gives it a speed at the end of its glide phase of either Mach 5 or Mach 9. The time of flight is indicated for the points shown.

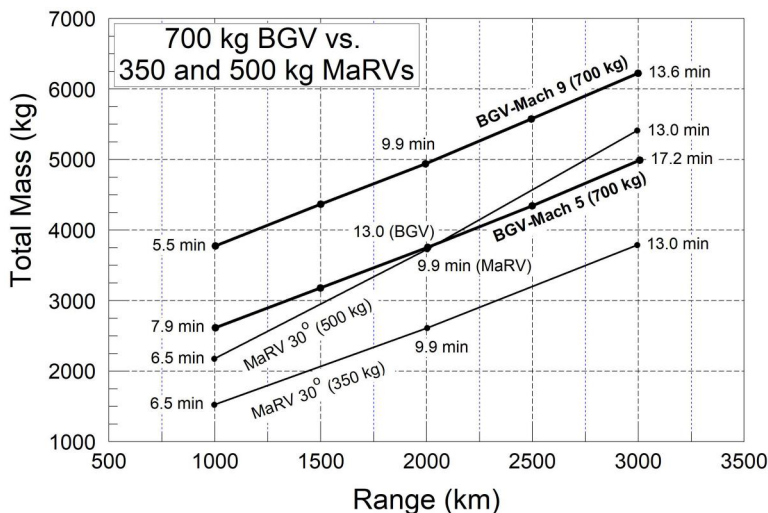


Figure 8. The results shown in Figure 7 for the case in which 350- and 500-kg MaRVs are compared to the 700-kg BGVs shown in that figure. The burnout speed of the MaRVs is the same as in Figure 7 so their total masses are reduced by the ratio of the MaRV vehicle masses in the two cases (350/700 and 500/700). the flight time versus range curves in Figure 9 still apply.

Implications of the results

Mach 5 case. Gliding increases the range of a BGV relative to a MaRV for the same burnout speed. While small for low total masses (around 2,500 kg) the range difference increases with total mass, assuming equal vehicle masses. For total masses around 5,000 kg, Figure 7 shows that the

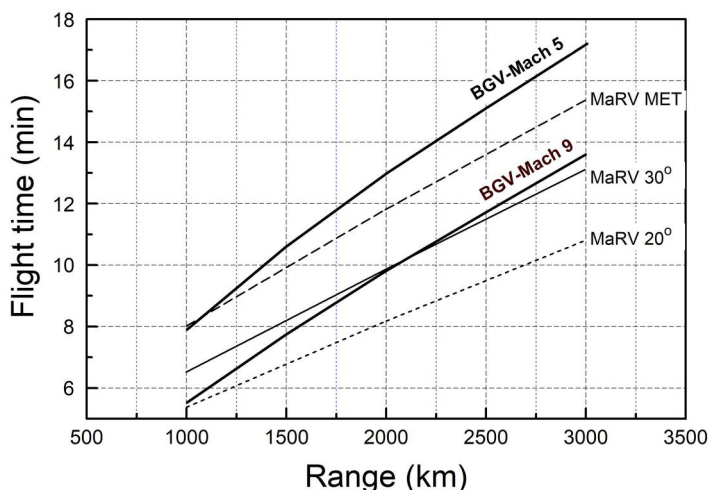


Figure 9. Flight time versus range for the scenarios described in Figures 7 and 8. The points correspond to the smallest total mass for each range and vehicle mass, as shown in Figures 7 and 8.

maximum BGV-5 range would be about 3,000 km compared to about 2,000 km for a MaRV with the same vehicle mass.

This difference can also be discussed in terms of the total masses of the two systems required to reach a given range. The mass difference is small for ranges less than 1,000 km. For 1,000 km maximum range the MaRV total mass is larger than that of a BGV-5 by about 15%; at 2,000 km it is larger by 35%, and at 3,000 km it is larger by 50%.

However, if the MaRV vehicle mass can be reduced by these percentages relative to the BGV, then both systems will have the same range for the same total mass (Figure 8 and Equation 8).

In addition, MaRVs can have significantly shorter flight times than BGV-5s to the same maximum range (Figure 9): The flight time of a BGV-5 is 20% longer than a MaRV with a 30° burnout angle over 1,000 km range and about 30% longer over ranges from 2,000 to 3,000 km.

Mach 9 case. The situation is different for BGVs diving at speeds high enough to evade terminal defenses.

As above, for systems with small total mass, MaRVs have a clear advantage over BGV-9s because they can have longer range at lower total mass, even assuming the MaRV and BGV vehicles have the same mass. Figure 4 shows that for the smallest total mass considered for a BGV-9 (3,000 kg) the MaRV range would be more than twice that of the BGV-9 because the starting glide velocity of the BGV-9 is not much above Mach 9, so it can glide only a short distance before it dives. If the MaRV vehicle mass can be reduced relative to that of the BGV, the MaRV's advantage is even greater (Figure 5).

For total masses of 4,500–5,000 kg, MaRVs and BGV-9s would have similar capabilities, (assuming equal vehicle masses) with ranges of 1,600–2,000 km (Figure 7). The MaRV could reach longer ranges if it had a smaller vehicle mass (Figure 8).

For ranges beyond 2,000 km the flight time of a MaRV launched with a 30° burnout angle to its maximum range would be less than that of a BGV-9 flying to the same range (Figure 9). Assuming equal vehicle masses, for 3,000 km maximum range the total mass of a MaRV would be about 25% larger than a BGV-9 (about 7,600 kg for the MaRV versus 6,200 kg for the BGV-9) (Figure 7). On the other hand, if the MaRV vehicle mass was 20% smaller than the BGV vehicle mass, both systems would have the same total mass for 3,000 km maximum range and the MaRV flight time would be shorter by half a minute.

Appendix B discusses how changing L/D affects these results.

The dynamics of maneuvering during glide phase

The ability to maneuver in midcourse is frequently cited as a significant advantage for BGVs over MaRVs.⁹¹ Reasons given include retargeting during flight; increasing the uncertainty of the trajectory to a defender; and avoiding overflight of certain regions from a given launch site, either for political reasons or to avoid a defense or radar site.

These benefits must be weighed against various considerations. For example, the fact that short-range systems can be launched from mobile platforms may reduce the importance of midcourse maneuvering. In addition, if BGVs can be detected by space-based sensors, maneuvering around ground-based radars may be of little utility. And while midcourse maneuvering can increase the area over which the weapon can be retargeted, maneuvering during reentry alone can allow either a BGV or MaRV to retarget over hundreds of kilometers.

Moreover, making large maneuvers in the glide phase can significantly reduce the speed and range of a BGV.⁹² Consider a BGV with speed V . To turn, it uses lift to generate a force perpendicular to its motion, creating a perpendicular velocity component V_{\perp} to change the direction of its velocity vector.

Because V is large, even relatively small turn angles require large V_{\perp} . For example, if $V = 4$ km/s (Mach 13.3) turning by just 25° requires creating a V_{\perp} of about 1.7 km/s (Mach 5.6), which is itself a hypersonic velocity.

To turn, the vehicle would bank and use some of its lift for changing directions rather than staying aloft. To do this, the vehicle would drop below its initial glide altitude during the turn. At the new altitude, the BGV would have essentially the same speed but at higher atmospheric density and could

use the additional lift to turn. Its drag would be greater than at its original altitude, which would reduce its speed and range relative to gliding without turning. We discuss this process and calculate the tradeoff.

Assume a BGV is gliding with speed V_1 at altitude h_1 and density $\rho_1 = \rho(h_1)$. It uses its entire lift force to stay aloft (see Equation 18):

$$F_L^{(1)} = \frac{C_L A \rho_1 V_1^2}{2} = \left(1 - \frac{V_1^2}{V_e^2}\right) mg \equiv \alpha(V_1) mg \quad (26)$$

where $V_e^2 = g(R_e + h)$. Equation 26 gives the density at the initial glide altitude as:

$$\rho_1 = \frac{2\alpha_1 mg}{C_L A V_1^2} = \frac{2\alpha_1 g \beta}{L/D V_1^2} \quad (27)$$

where $\alpha_1 = \alpha(V_1)$. For altitudes of interest here h and ρ are related by:⁹³

$$\rho(h) = 1.75 \exp\left(-\frac{h}{6.7}\right) \quad (28)$$

with h in km and ρ in kg/m^3 . The density increases by about a factor of two for each 5 km drop in altitude.

Assume that the BGV drops instantaneously from h_1 to h_2 to begin its turn and banks by angle θ to create a horizontal component of lift. It flies for a pathlength r at the lower altitude and then stops banking and uses its lift to rise instantaneously to its new glide altitude, which will be somewhat lower than h_1 because its speed has decreased during the turn.⁹⁴

When the vehicle drops to h_2 , the speed is assumed initially to remain at V_1 , so the vertical force keeping the vehicle aloft at h_2 is:

$$F_v^{(2)} = F_L^{(2)} \cos \theta = \frac{C_L A \rho_2 V_1^2}{2} \cos \theta = \alpha_1 mg \quad (29)$$

where $F_L^{(2)}$ is the total lift force at h_2 and the last equality uses the fact that the vertical component of lift must keep the vehicle aloft with speed V_1 at the new altitude (ignoring the small change in V_e due to this small change in altitude). Since $F_L^{(1)} = \alpha_1 mg$, then Equations 26 and 29 give:

$$\cos \theta = \frac{\rho_1}{\rho_2} \quad (30)$$

where θ is the bank angle.⁹⁵

During the turn, drag will slow the vehicle. Since the vertical force $F_v^{(2)}$ must remain equal to $\alpha(V)mg$, the vehicle slowly drops in altitude to increase the ambient density:

$$F_v^{(2)}(V) = F_L^{(2)}(V) \cos \theta = \frac{C_L A \rho V^2}{2} \cos \theta = \alpha(V) mg \quad (31)$$

The horizontal force used for turning is:

$$F_{\perp}(V) = F_L^{(2)} \sin \theta = F_v^{(2)} \tan \theta = \alpha(V)mg \tan \theta \quad (32)$$

The drag during the turn is:

$$F_D^{(2)} = \frac{C_D A \rho V^2}{2} = \frac{\alpha(V)mg}{L/D \cos \theta} \quad (33)$$

where the last equality uses [Equation 31](#).

[Equation 33](#) shows that the drag is larger than at the original altitude by a factor that reflects the ratio of densities ([Equation 30](#)), as expected. The change in speed that results from the BGV flying at the lower altitude over a distance r , starting at a speed V_I at a bank angle θ , is given by [Equation 22](#) with the drag force increased by a factor of $1/\cos \theta$:

$$V(r) = V_e [1 - \alpha_1 \exp(r/R_\theta)]^{1/2} \quad (34)$$

where

$$R_\theta \equiv \frac{L/D \cos \theta V_e^2}{2g} \quad (35)$$

F_{\perp} creates a lateral horizontal velocity V_{\perp} . Since F_{\perp} always acts perpendicular to V it will rotate V but not change its magnitude, rotating it by an angle κ , which can be calculated using:

$$d\kappa = \frac{dV_{\perp}}{V(r)} = \frac{1}{V} \frac{F_{\perp}}{m} dt = \frac{\alpha(V)g \tan \theta}{V} dt = \frac{\alpha(V)g \tan \theta}{V^2} dr \quad (36)$$

since $dV_{\perp} = (F_{\perp}/m) dt$, and using [Equation 32](#) and the fact that $dt = dr/V$. Inserting [Equation 34](#) for V and integrating gives:

$$\int_0^{\kappa} d\kappa' = \frac{g \tan \theta}{V_e^2} \left[-r + \int_0^r \frac{dr'}{1 - \alpha_1 \exp(r'/R_\theta)} \right] \quad (37)$$

which gives:

$$\kappa(r) = \frac{L/D \sin \theta}{2} \ln \left(\frac{1 - \alpha_1}{1 - \alpha_1 \exp(r/R_\theta)} \right) \quad (38)$$

[Equation 38](#) gives the angle of rotation for a BGV gliding over a distance r starting at a speed V_I and with a constant bank angle θ .

The radius of curvature of the turn is given by:

$$Radius_{turn} = \frac{r}{\kappa} \quad (39)$$

[Equation 38](#) gives the distance r the vehicle must travel at lower altitudes to turn by κ before returning to higher altitudes to glide with $\theta = 0$.

The distance r required for a given κ decreases as θ increases, i.e., the vehicle turns faster at lower altitudes where the atmospheric is thicker.

The time required for this turn (traveling a distance r , starting at a speed V_I at bank angle θ) is given by Equation 24 with the drag force increase by $1/\cos \theta$:

$$t(r) = \frac{r}{V_e} - \frac{2R_\theta}{V_e} \ln \left[1 + \left(\frac{1 - \alpha_1 \exp(r/R_\theta)^{1/2}}{1 + V_I/V_e} \right) \right] \quad (40)$$

The additional drag the vehicle experiences while at lower altitudes will decrease the speed and the maximum range of the BGV compared to remaining at its original altitude without turning. The decrease in V from its initial speed V_I while traveling the distance r during the turn, compared to traveling the same distance r starting at the original altitude, is given by (using Equations 22 and 34):

$$\delta V(r) = V_e \left(\left[1 - \alpha_1 \exp \left(\frac{2\alpha_1 g r}{L/D V_e^2} \right) \right]^{1/2} - \left[1 - \alpha_1 \exp \left(\frac{2\alpha_1 g r}{L/D V_e^2 \cos \theta} \right) \right]^{1/2} \right) \quad (41)$$

We can similarly compare the total pathlength of the glide phases of the maneuvering and non-maneuvering flights. If the BGV begins its maneuver with speed V_I then Equation 34 gives its speed V_2 after maneuvering over a distance r . Its total glide distance, assuming glide ends when it reaches V_f is:

$$R_G^m(r, V_f) = r + \frac{L/D V_e^2}{2g} \ln \left(\frac{1 - V_f^2/V_e^2}{1 - V_2^2/V_e^2} \right) \quad (42)$$

where the first term is the glide distance during the turn and the second term is Equation 23 for the glide distance when the banking angle is set to zero after maneuvering.

This pathlength can be compared to the BGV range starting with a speed V_I and flying until it reaches V_f without maneuvering:

$$R_G^0(0, V_f) = \frac{L/D V_e^2}{2g} \ln \left(\frac{1 - V_f^2/V_e^2}{1 - V_I^2/V_e^2} \right) \quad (43)$$

Figures 10–14 illustrate the dynamics of turning at two speeds and angles (assuming $L/D=2.6$). We determine the turn distance r required to give a turn angle κ for a given altitude change δh , and calculate the time duration of the turn, the velocity change, and distance traveled.

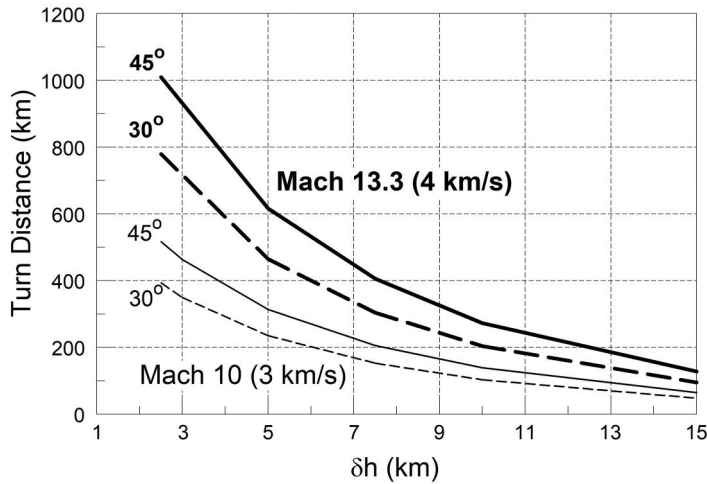


Figure 10. The pathlength the BGV must travel at an altitude δh below its initial glide altitude for the turns shown (30° for the dotted curves and 45° for the solid curves). The bold lines are for an initial BGV speed $V_i = \text{Mach } 13.3$ and the thin lines are for $V_i = \text{Mach } 10$. The total glide range with no maneuvering is 980 km for $V_i = \text{Mach } 10$ and 2,140 km for Mach 13.3 (in both cases gliding to $V_f = \text{Mach } 5$), for the parameters used here ($L/D = 2.6$).

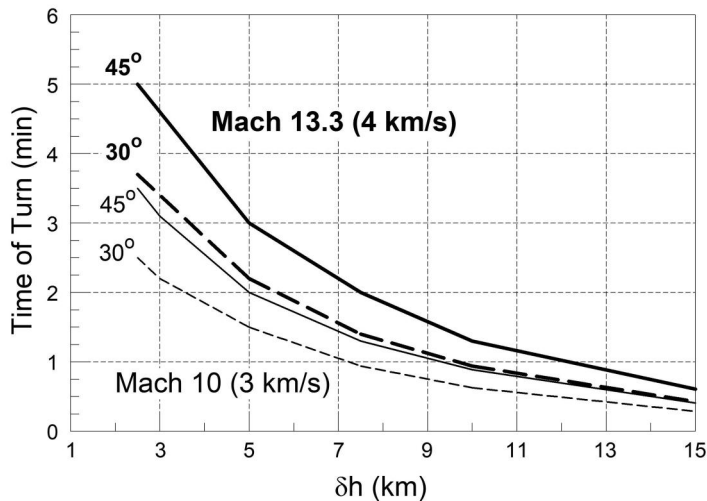


Figure 11. The time required for the BGV to turn through the angles of 30° and 45° by dropping in altitude by a distance δh during the turn. Other details as in Figure 10.

Implications

These plots show that midcourse maneuvering can be slow and costly. Turning at altitudes only a few kilometers below the equilibrium glide altitude can reduce the costs but will be slow and take place over a third to a half of the total glide range for turn angles of 30° – 45° .

Faster turns over a shorter distance require dropping to lower altitudes for the maneuver, which can significantly reduce the glide range (Figures 13

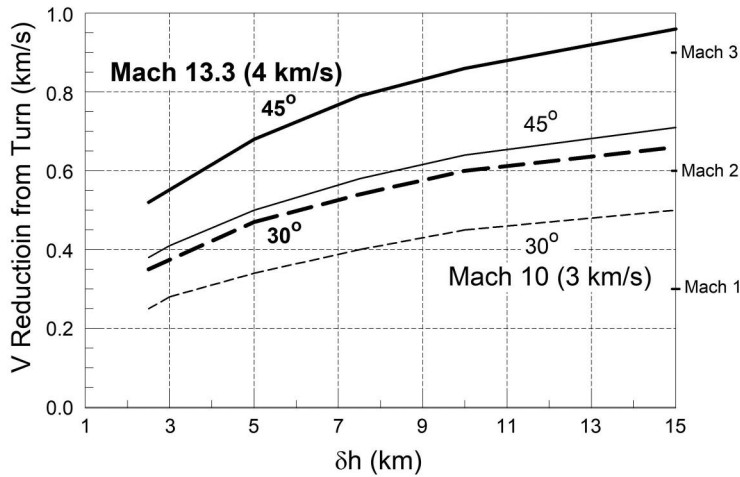


Figure 12. Decrease in BGV speed resulting from turns, relative to the speed it would have after traveling the same distance without turning. Speed reductions are shown in km/s on the left axis and Mach numbers on the right axis. Other details as in Figure 10.

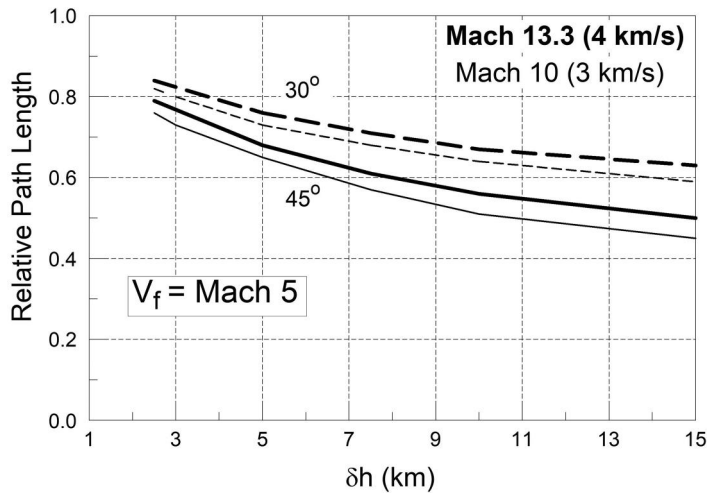


Figure 13. Reduction in BGV pathlength due to turning, for $V_f = \text{Mach } 5$. Curves show the total glide range of the maneuvering BGV divided by its range had it remained at its initial equilibrium glide altitude without turning. Other details as in Figure 10.

and 14), especially for BGVs intended to evade defenses (Figure 14). In this case BGVs starting their turns at Mach 10 will have very short glide ranges.

The discussion above is for a single turn. Maneuvering around a particular location may require multiple turns, which can significantly increase the costs.

For example, consider a BGV at Mach 10 that makes a 30° turn by reducing its altitude by 5 km, and then turns by -30° to return to its initial heading (Figure 15). The BGV will travel 235 km during the first turn, and its speed will drop to 2.4 km/s. Turning back by 30° will require it to travel

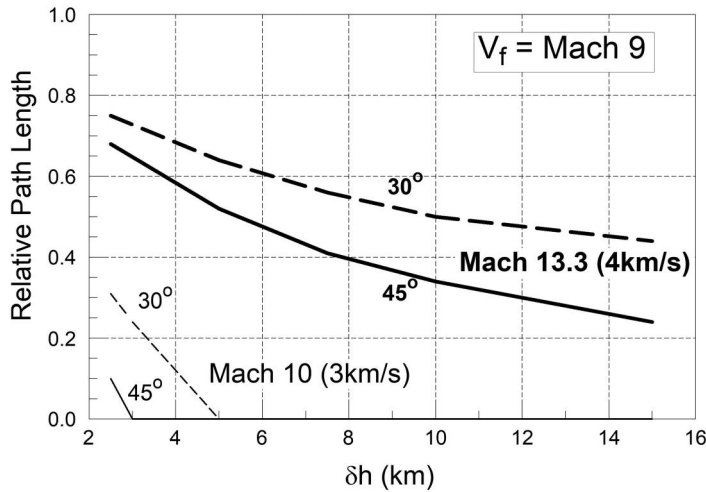


Figure 14. Reduction in BGV path length due to turning as in Figure 13, but for $V_f = \text{Mach } 9$.

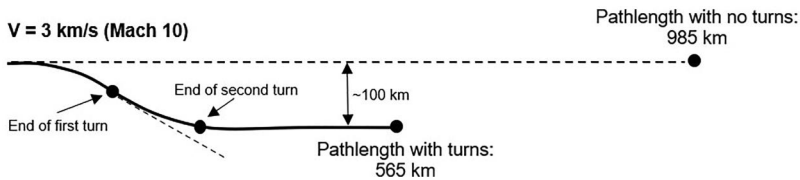


Figure 15. The trajectory of a BGV initially traveling at Mach 10 that dives from its glide when $V_f = \text{Mach } 5$. To turn, it drops by $\delta h = 5 \text{ km}$, turns by 30° clockwise and then by 30° counter-clockwise to its original heading, after which it returns to its (new) equilibrium glide altitude. The increased drag reduces the total glide pathlength to 57% of its value with no turns, shown by the dashed line. This figure assumes $L/D = 2.6$.

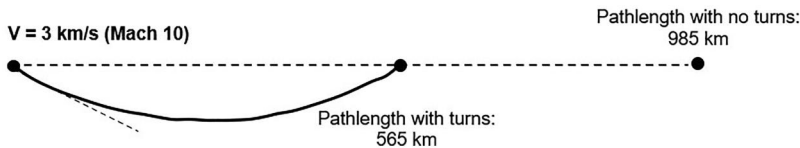


Figure 16. A maneuver similar to that in Figure 15 except the BGV is initially launched 30° from the line to the target, and maneuvers by 60° to reach the target. As in Figure 15, the increased drag reduces its total glide pathlength to about 57% of the pathlength it would have with no turns, shown by the dashed line.

140 km and its speed will be 1.9 km/s when it returns to its equilibrium glide altitude. From there it could travel only 190 km until reaching Mach 5. Its total glide pathlength will be only about 565 km rather than 985 km without turning. In this case the new trajectory has only moved laterally by about 100 km.

In Figure 16, the BGV is launched 30° from the direction to the intended target to fly around a location on a line between the two. This case is the same as in Figure 15, but with both turns in the same direction. The total

pathlength of the maneuvering case is again 565 km, compared with 985 km with no maneuvering. If the BGV needed to reach a greater distance from the dotted line during the maneuver, that would require larger turns which would further reduce its range.

Conclusions

U.S. development of BGVs and the decision to procure and deploy these weapons appear to have proceeded without a careful analysis of whether their military missions can be met as well or better using other systems, especially those that may be less expensive and more reliable since they rely largely on existing technologies.

Since U.S. BGV development focuses on systems with glide ranges less than about 1,500 km and total ranges less than about 3,000 km, this paper compares those systems to MaRVs flying on depressed trajectories.

Hypersonic weapons and terminal defenses

Our analysis of current terminal missile defenses shows that hypersonic weapons of the types considered here may be vulnerable to endo-atmospheric interceptors when the BGV or MaRV are in the final dive portions of their trajectories. A key result is that evading current missile defense systems requires vehicles to maintain speeds substantially higher than Mach 5 throughout their glide.

In particular, the speed of a reentering vehicle throughout its dive to the target should be greater than that of the interceptor. To evade the most capable current defense systems, a BGV or MaRV must maintain a speed greater than about Mach 6 during its dive, meaning that a BGV should begin its dive from glide phase with a speed of about Mach 10 or greater.

Moreover, the required minimum speed of a BGV will increase as new generations of faster endo-atmospheric defenses are developed.

Because of the velocity losses of the BGV during pull-up and glide phases, a BGV requires a higher burnout speed than a MaRV to achieve the same speeds during reentry.

Range, flight time, and mass of BGVs vs. MaRVs

The total mass and size of the BGV or MaRV vehicle plus booster is important for some basing modes. This analysis estimates the minimum total masses of BGVs and MaRVs as a function of range. (Range here refers to the total range of the weapon after booster burnout.) While the specific results of the calculations depend on the particular parameter values assumed for the vehicles, our calculations illustrate the relative capabilities and potential tradeoffs between two systems with the same parameter values.

Our baseline comparison assumes that the BGV and MaRV use the same vehicle flown on different trajectories. We also look at MaRVs that are less massive than a BGV vehicle.

The primary advantage of BGVs is their ability to fly at low altitudes for long distances, which is primarily useful for maneuvering during midcourse flight. While it can also allow them to underfly exo-atmospheric missile defenses, U.S. weapons of the ranges considered here are unlikely to face exo-atmospheric defenses in the foreseeable future. Our analysis shows that these BGV capabilities come at a cost in speed, mass, and/or range, as well as increased heat loading.

Our results show there are important missions in which MaRVs have a combination of mass and delivery time that make them preferable to BGVs, especially if MaRV vehicles can be made less massive than BGVs. A general advantage of MaRVs is that they use existing technologies and are not subject to the prolonged, intense heating or aerodynamic instabilities of a BGV's glide phase, which have complicated and slowed the development of BGVs. MaRVs may therefore be available sooner, be less expensive, and have higher reliability than BGVs.

Our analysis compares the capabilities of MaRVs with BGVs that finish their glide phase with speeds of either Mach 9 or Mach 5; the former may be able to evade current terminal defenses, while the latter likely cannot. We refer below to these as BGV-9 and BGV-5, respectively.

BGVs that can evade defenses (BGV-9). Our results show that if launch vehicles, such as aircraft, only carry weapons with masses less than about 3,000 kg, then MaRVs have a clear advantage over BGV-9s.

In particular, for these masses, aircraft would not carry a BGV-9 with a range of more than a few hundred kilometers unless the BGV vehicle mass was less than 700 kg. Such aircraft could, however, launch a 700-kg MaRV vehicle from a range of about 1,000 km that could maintain speed sufficient to evade terminal defenses. Lower mass MaRV vehicles could be launched from significantly greater distances.

Weapons with total mass greater than about 3,000 kg are likely to be launched from land or sea, and the mass and size of the weapon is likely to be less of a consideration.

Assuming equal vehicle masses, for ranges up to about 1,750 km a MaRV can have a lower total mass than a BGV-9. For longer ranges, a BGV-9 will have a smaller total mass than a MaRV for comparable flight time.

If, however, the MaRV vehicle mass is 20% less than the mass of the BGV vehicle, the total mass of the MaRV will be less than that of the BGV-9 over all the ranges considered here.

BGVs not intended to evade defenses (BGV-5). If BGVs are intended to have hypersonic speeds but not evade terminal defenses, i.e., maintain glide speeds above Mach 5 but below Mach 9, then a BGV could reach longer ranges than a MaRV with the same burnout speed for ranges longer than about 500 km.

For small total masses, the range difference is small: A BGV-5 with a total mass of 2,500 kg could have a range up to about 900 km compared to about 800 km for a MaRV of the same mass. If, however, the MaRV vehicle mass could be reduced by 10% it could also reach 900 km range for the same total mass and same flight time as the BGV-5. Further reductions in MaRV mass relative to the BGV would make MaRV capabilities competitive with those of the BGV-5 at longer ranges.

The difference in capabilities of the systems increases with range and total mass. For ranges of 2,000–3,000 km, assuming the vehicles have the same mass, the total mass of a MaRV would be larger than that of a BGV-5 by 35–50%, since it would require a higher burnout speed, but the delivery time would be 30% shorter. If the MaRV vehicle mass could be made 25–35% smaller than the BGV vehicle mass, the two systems would have the same range for the same total mass at these ranges.

Maneuvering

Both MaRVs and BGVs can maneuver aerodynamically by hundreds of kilometers during their final reentry. In addition, BGVs can maneuver during their glide phases, and some proponents cite this additional maneuvering capability as an important advantage.

Midcourse maneuvering, however, increases drag and can significantly reduce the BGV's speed and range, which limits the potential amount of maneuvering and therefore reduces the advantages of such maneuvering. In comparing BGVs with MaRVs, one must therefore take into account the potential costs and benefits of midcourse maneuvering and the scenarios in which it might be important.

Notes and References

1. The speed of sound in the atmosphere varies by about 10% over the range of altitudes of interest for BGVs (10–50 km). We assume a speed of 300 m/s, which is roughly consistent with a standard engineering approximation that uses 1000 ft/s as sound speed at these altitudes. See “1976 Standard Atmosphere Calculator,” DigitalDutch, <https://www.digitaldutch.com/atmoscalc/table.htm>.
2. Richard H. Speier, George Nacouzi, Carrie A. Lee, and Richard M. Moore, *Hypersonic Missile Nonproliferation: Hindering the Spread of a New Class of Weapons* (Santa

- Monica, CA: RAND Corporation, 2017), 53–93, https://rand.org/pubs/research_reports/RR2137.html.
3. MaRVs were developed and tested during the Cold War and in the 2000s. See Matthew Bunn, “Technology of Ballistic Missile Reentry Vehicles,” in *Review of U.S. Military Research and Development: 1984*, eds. Kosta Tsipis and Penny Janeway (McLean, VA: Pergamon, 1984), 87–107, https://scholar.harvard.edu/files/bunn_tech_of_ballistic_missile_reentry_vehicles.pdf. See also National Research Council, *U.S. Conventional Prompt Global Strike: Issues for 2008 and Beyond*, Committee on Conventional Prompt Global Strike Capability (2008), <https://doi.org/10.17226/12061>, and Amy Woolf, *Conventional Prompt Global Strike and Long-Range Ballistic Missiles: Background and Issues* (Washington, DC: Congressional Research Service, 2021), <https://crsreports.congress.gov/product/pdf/R/R41464>.
 4. James M. Acton, “Hypersonic Boost-Glide Weapons,” *Science and Global Security* 23 (2015): 191–219, <http://scienceandglobalsecurity.org/archive/sgs23acton.pdf>; David Wright, “Research Note to Hypersonic Boost-Glide Weapons by James M. Acton: Analysis of the Boost Phase of the HTV-2 Hypersonic Glider Tests,” *Science and Global Security* 23 (2015): 220–9, <http://scienceandglobalsecurity.org/archive/sgs23wright.pdf>.
 5. Cameron L. Tracy and David Wright, “Modelling the Performance of Hypersonic Boost-Glide Missiles,” *Science and Global Security* 28 (2021): 135–170, <http://scienceandglobalsecurity.org/archive/sgs28tracy.pdf>. This paper uses a different coordinate system for the equations of motion than is used in many papers. That system and the reasons behind it are described in [Appendix A](#).
 6. “The First Missile Regiment of Avangard Took Up Combat Duty,” TASS, December 27, 2019, <https://tass.ru/armiya-i-opk/7436431>; “Deployment of Avangard continues in Dombrovskiy,” Russian Strategic Nuclear Forces, December 16, 2020, https://russianforces.org/blog/2020/12/deployment_of_avangard_continu.shtml.
 7. “Avangard,” Center for Strategic and International Studies, July 31, 2021, <https://missilethreat.csis.org/missile/avangard/>.
 8. An additional motivation appears to be a desire to match work on hypersonic weapons by Russia and China. See, for example, Oren Liebermann, “US is Increasing Pace of Hypersonic Weapons Development to Chase China and Russia, Senior Admiral Says,” CNN, November 20, 2022, <https://www.cnn.com/2022/11/20/politics/us-hypersonic-china-russia-competition/index.html>.
 9. Ivett A. Leyva, “The Relentless Pursuit of Hypersonic Flight,” *Physics Today*, 70 (2017): 30–6, <https://doi.org/10.1063/PT.3.3762>.
 10. See, for example, Joseph Trevithick, “Here’s How Hypersonic Weapons Could Completely Change the Face of Warfare,” *The War Zone*, June 6, 2017, <https://www.thedrive.com/the-war-zone/11177/heres-how-hypersonic-weapons-could-completely-change-the-face-of-warfare>; Benjamin Knudsen, “An Examination of U.S. Hypersonic Weapon Systems,” Technical Report, George Washington University, June 2017, DOI:10.13140/RG.2.2.14375.96164; “Hypersonic Strike and Defense: A Conversation with Mike White,” *Center for Strategic and International Studies*, June 10, 2021, <https://www.csis.org/analysis/hypersonic-strike-and-defense-conversation-mike-white>. Another possible motivation, reducing warning of an attack by avoiding detection, does not appear to be as central. Ground-based radars will not see a BGV during glide until it is within about 500 km, but this may not be particularly relevant. This range should still provide time to launch short-range interceptors against it. For high-value targets, forward-basing radars would provide additional warning time.

- Moreover, U.S. and Russian space-based infrared (IR) sensors (which China is developing) can provide early warning of the launch of the boosters carrying BGVs and can also detect IR emissions from BGVs gliding at sufficiently high speeds, providing warning and cuing information even if this data is not sufficient to guide interceptors (see Paper 1).
11. This paper focuses on terminal defenses for several reasons, discussed in detail below. BGVs can underfly midcourse (exo-atmospheric) defenses, which appears to be a motivation for Russia's development of the Avangard HGV, but this paper focuses on shorter range BGVs used for conventional conflict.
 12. Congressional Budget Office (CBO), "U.S. Hypersonic Weapons and Alternatives," January 2023, <https://www.cbo.gov/publication/58255>.
 13. See Paper 1 and analysis below.
 14. CBO, "U.S. Hypersonic Weapons."
 15. Acton, "Hypersonic Boost-Glide Weapons."
 16. "Minimum-energy trajectories" give the maximum range for a given burnout speed and altitude.
 17. Lisbeth Gronlund and David Wright "Depressed-Trajectory SLBMs: A Technical Assessment and Arms Control Possibilities," *Science and Global Security* 3 (1992): 101–59, <http://scienceandglobalsecurity.org/archive/sgs03gronlund.pdf>.
 18. Press reports also reflect this ambiguity. Russia's Kinzhal system used against Ukraine is a maneuvering air-launched ballistic missile rather than a BGV (Kelley Saylor, *Hypersonic Weapons: Background and Issues for Congress* (Washington, DC: Congressional Research Service, 2023), <https://crsreports.congress.gov/product/pdf/R/R45811>). The "hypersonic weapon" North Korea has reportedly tested is also described this way (Iain Marlow and Jon Herskovitz, "Kim Jong Un's Hypersonic Missiles Show He Can Hit U.S. Back," *Bloomberg*, January 12, 2022, <https://www.bloomberg.com/news/articles/2022-01-12/kim-jong-un-s-new-hypersonic-missiles-show-he-can-hit-u-s-back>).
 19. Richard Hallion, "The History of Hypersonics: or, 'Back to the Future—Again and Again'," American Institute of Aeronautics and Astronautics, AIAA-2005-329 (2005), 43rd AIAA Aerospace Sciences Meeting and Exhibit, 10–13 January 2005, Reno, NV, <https://doi.org/10.2514/6.2005-329>.
 20. Woolf, *Conventional Prompt Global Strike*.
 21. Acton, "Hypersonic Boost-Glide Weapons."
 22. "An Historical Overview of Waverider Evolution," Staar Research, <https://www.gbnet.net/orgs/staar/wavehist.html>.
 23. Research is being done on BGVs designed to optimize lift at more than one velocity; see, e.g., Zhen-tao Zhao, Wei Huang, Li Yan, Yan-guang Yang, "Overview of Wide-speed Range Waveriders," *Progress in Aerospace Sciences* (2020) 113: 1–14, <https://doi.org/10.1016/j.paerosci.2020.100606>.
 24. Acton, "Hypersonic Boost-Glide Weapons." Plans called for the HTV-2 to have L/D of 3.5 to 4 and the HTV-3 to have L/D of 4 to 5. The program was terminated before HTV-3 was produced.
 25. Woolf, *Conventional Prompt Global Strike*.
 26. Kenneth W. Iloff and Mary F. Shafer, "A Comparison of Hypersonic Flight and Prediction Results," *American Institute of Aeronautics and Astronautics*, AIAA-93-0311 (1993), 31st Aerospace Sciences Meeting and Exhibit, 11–14 January 1993, Reno, NV, <https://doi.org/10.2514/6.1993-311>.
 27. Woolf, *Conventional Prompt Global Strike*, 17.

28. “Advanced Hypersonic Weapon,” *Army Technology*, April 10, 2012, <https://www.army-technology.com/projects/advanced-hypersonic-weapon-ahw/> The Army reportedly tested a “downscaled version” in October 2017 (Sydney J. Freedberg, Jr., “Army Warhead Is Key to Joint Hypersonics,” *Breaking Defense*, August 22, 2018, <https://breakingdefense.com/2018/08/army-warhead-is-key-to-joint-hypersonics/>).
29. Acton, “Hypersonic Boost-Glide Weapons.”
30. Joseph Trevithick, “USAF, Army, and Navy Join Forces to Field America’s First Operational Hypersonic Weapon,” *The Drive*, October 11, 2018, <https://www.thedrive.com/the-war-zone/24181/usaf-army-and-navy-join-forces-to-field-americas-first-operational-hypersonic-weapon>.
31. John A. Tirpak, “Air Force Cancels HCSW Hypersonic Missile in Favor of ARRW,” *Air Force Magazine*, February 10, 2020, <https://www.airforcemag.com/air-force-cancels-hcsw-hypersonic-missile-in-favor-of-arrw/>.
32. CBO, “U.S. Hypersonic Weapons.”
33. Yi Feng, Shenshen Liu, Wei Tang, Yewei Gui, “Aerodynamic Configuration Design and Optimization for Hypersonic Vehicles, *American Institute of Aeronautics and Astronautics* (2017), 21st AIAA International Space Planes and Hypersonics Technologies Conference, 6–9 March 2017, Xiamen, China, <https://doi.org/10.2514/6.2017-2173>; The analysis in Appendix G of National Research Council, U.S. *Conventional Prompt Global Strike*, 206–215, assumes $L/D = 2.2$ for its calculations.
34. Joseph Trevithick, “The Army and Navy Have Conducted the First Joint Test of Their New Hypersonic Weapon,” *The Drive*, March 20, 2020, <https://www.thedrive.com/the-war-zone/32667/the-army-and-navy-have-conducted-the-first-joint-test-of-their-new-hypersonic-weapon>, Caleb Larson, “This U.S. Missile Can Kill Any Target on the Planet (In Less Than an Hour),” *National Interest*, June 23, 2020, <https://nationalinterest.org/blog/buzz/us-missile-can-kill-any-target-planet-less-hour-163303>.
35. Saylor, *Hypersonic Weapons*.
36. John A. Tirpak, “Roper: The ARRW Hypersonic Missile Better Option for USAF,” *Air Force Magazine*, March 2, 2020, <https://www.airforcemag.com/arrw-beat-hcsw-because-its-smaller-better-for-usaf/>.
37. Stephen Losey, “US Air Force drops Lockheed hypersonic missile after failed tests,” *Defense News*, March 30, 2023, <https://www.defensenews.com/air/2023/03/30/us-air-force-drops-lockheed-hypersonic-missile-after-failed-tests/>.
38. Guy Norris, “High-Speed Strike Weapon to Build on X-51 Flight,” *Aviation Week & Space Technology*, May 20, 2013, https://web.archive.org/web/20140104023933/http://www.aviationweek.com/Article/PrintArticle.aspx?id=/article-xml/AW_05_20_2013_p24-579062.xml&p=1&printView=true.
39. “X-51A Waverider,” U.S. Air Force Factsheet, May 3, 2013, <https://web.archive.org/web/20130619105330/http://www.af.mil/information/factsheets/factsheet.aspx?fsID=17986>; “Hyper-X Program,” NASA Factsheet, February 28, 2014, <https://www.nasa.gov/centers/armstrong/news/FactSheets/FS-040-DFRC.html>.
40. Kristen N. Roberts, *Analysis and Design of a Hypersonic Scramjet Engine with a Starting Mach Number of 4.00*, Master’s thesis in Aerospace Engineering, University of Texas at Arlington, 2008, <http://hdl.handle.net/10106/1073>.
41. Sydney J. Freedberg, Jr., “Hypersonics: DoD Wants ‘Hundreds of Weapons’ ASAP,” *Breaking Defense*, April 24, 2020, <https://breakingdefense.com/2020/04/hypersonics-dod-wants-hundreds-of-weapons-asap/>.
42. Saylor, *Hypersonic Weapons*.

43. “Kh-47M2 Kinzhal,” *Missile Threat*, 19 March 2022, <https://missilethreat.csis.org/missile/kinzhal/#easy-footnote-bottom-10-3801>. The Kinzhal mass is estimated as 3,800 kg (Vladimir Karnozov, “Putin Unveils Kinzhal Hypersonic Missile,” *AIN Online*, March 2, 2018, <https://www.ainonline.com/aviation-news/defense/2018-03-02/putin-unveils-kinzhal-hypersonic-missile>).
44. Franz-Stefan Gady, “China Tests New Weapon Capable of Breaching US Missile Defense Systems,” *The Diplomat*, April 28, 2016, <https://thediplomat.com/2016/04/china-tests-new-weapon-capable-of-breaching-u-s-missile-defense-systems/>; Sayler, “Hypersonic Weapons.”
45. Mike Yeo, “China unveils drones, missiles and hypersonic glide vehicle at military parade,” *Defense News*, October 1, 2019, <https://www.defensenews.com/global/asia-pacific/2019/10/01/china-unveils-drones-missiles-and-hypersonic-glide-vehicle-at-military-parade/>.
46. Zhao Lei, “Superfast aircraft test a ‘success’,” *China Daily*, August 6, 2018, <http://usa.chinadaily.com.cn/a/201808/06/WS5b6787b4a3100d951b8c8ae6.html>.
47. Sayler, *Hypersonic Weapons*.
48. These values vary slowly with L/D and β . For $L/D = 6$, they would be 34 km at Mach 5 and 44 km at Mach 10.
49. Thomas Newdick, “This Is Our First View of Russia’s New S-500 Air Defense System In Action,” *The Drive*, July 20, 2021, <https://www.thedrive.com/the-war-zone/41627/this-is-our-first-view-of-russias-new-s-500-air-defense-system-in-action>.
50. Andrew M. Sessler, John M. Cornwall, Bob Dietz, Steve Fetter, Sherman Frankel, Richard L. Garwin, Kurt Gottfried, Lisbeth Gronlund, George N. Lewis, Theodore A. Postol, et al., *Countermeasures: The Operational Effectiveness of the Planned US National Missile Defense System* (Cambridge, MA: Union of Concerned Scientists and MIT Security Studies Program, April 2000), 28, <https://www.ucsusa.org/sites/default/files/2019-09/countermeasures.pdf>.
51. Ibid.
52. Theodore A. Postol and George N. Lewis, “The Illusion of Missile Defense: Why THAAD Will Not Protect South Korea,” *Global Asia* 11, no. 3 (2016): 80–5, <https://www.globalasia.org/data/file/articles/78a89c3da89bc3fae2f1e8249871c58e.pdf>.
53. “Theater High Altitude Area Defense (THAAD),” Aerojet Rocketdyne, March 13, 2019, <https://rocket.com/defense/missile-defense/thaad>.
54. For a discussion of acceleration saturation effects for various types of guidance, with and without lags, see Paul Zarchan, *Tactical and Strategic Missile Guidance - An Introduction*, 7th ed. (Reston, VA: American Institute of Aeronautics and Astronautics, Inc., 2019), Vol.1: 157–60, 206–11, 216–23, 254; Vol. 2: 165–7, 552–3. See also N. F. Palumbo, R. A. Blauwkamp, and J. M. Lloyd, “Modern Homing Missile Guidance Theory and Techniques,” *Johns Hopkins APL Technical Digest*, 29 (2010): 42–59, https://www.jhuapl.edu/Content/techdigest/pdf/V29-N01/29-01-Palumbo_Homing.pdf.
55. Zarchan, *Tactical and Strategic Missile Guidance*, 1: 152; 2: 147, 307, 439.
56. Angle-of-attack can be created using fins or small thrusters on the missile or interceptor body.
57. Zarchan, *Tactical and Strategic Missile Guidance*, 1: 157.
58. Lockheed Martin, “PAC-3 MSE Overview,” January 5, 2022, https://www.lockheedmartin.com/content/dam/lockheed-martin/mfc/documents/pac-3/2022-01-05_LM_PAC-3_MSE_Overview.pdf.

59. Terry H. Phillips, "A Common Aero Vehicle (CAV) Model, Description, and Employment Guide," Schafer Corporation (January 27, 2003).
60. Jon Hawkes "Patriot games: Raytheon's Air-Defence System Continues to Proliferate," *Jane's International Defence Review* 52 (2019): 1–6, https://web.archive.org/web/20190601000000/https://www.raytheon.com/sites/default/files/2018-12/Raytheon_article%20reprint_IDR%201901.pdf.
61. Office of the Director, Operational Test and Evaluation, "DOT&E FY 2016 Annual Report: Patriot Advanced Capability-3 (PAC-3)," December 2016, 175–7, <https://www.dote.osd.mil/Portals/97/pub/reports/FY2016/army/2016patriot.pdf?ver=2019-08-22-105407-280>; Isaac Maw, "Patriot Missile to Receive \$133M in Upgrades Over Next Five Years," *engineering.com*, July 9, 2018, <https://www.engineering.com/story/patriot-missile-to-receive-133m-in-upgrades-over-next-five-years>.
62. Patrick O'Reilly, Ed Waters, "The Patriot PAC-3 Missile Program—An Affordable Integration Approach," <https://apps.dtic.mil/sti/pdfs/ADA319957.pdf>; Missile Defense Project, "Patriot," *Missile Threat*, Center for Strategic and International Studies, June 14, 2018, <https://missilethreat.csis.org/system/patriot/> (last modified March 24, 2022).
63. Missile Defense Advocacy Alliance (MDAA), "Patriot Advanced Capability-3 Missile," August 18, 2020, <https://missiledefenseadvocacy.org/defense-systems/patriot-advanced-capability-3-missile/>. This speed is consistent with a recent article giving a maximum speed of existing interceptors as "about 1.7 km/s" ("Japan set to develop railguns to counter hypersonic missiles," *NIKKEI Asia*, January 4, 2022, <https://asia.nikkei.com/Politics/Japan-set-to-develop-railguns-to-counter-hypersonic-missiles>).
64. North Atlantic Treaty Organization (NATO), "Patriot," Fact Sheet, December 2012, https://www.nato.int/nato_static/assets/pdf/pdf_2012_12/20121204_121204-factsheet-patriot-en.pdf; MDAA, "Patriot."
65. Leland H. Jorgensen, "Prediction of Static Aerodynamic Characteristics for Space-Shuttle-Like and Other Bodies at Angles of Attack from 0° to 180°," NASA Report TN D-6996 (1973), <https://ntrs.nasa.gov/api/citations/19730006261/downloads/19730006261.pdf>.
66. Jorgensen, "Prediction of Static Aerodynamic Characteristics."
67. Leland H. Jorgensen, "A Method for Estimating Static Aerodynamic Characteristics for Slender Bodies of Circular and Noncircular Cross Sections," NASA Report TN 0-7228 (1973), <https://ntrs.nasa.gov/api/citations/19730012271/downloads/19730012271.pdf>.
68. Acton, "Hypersonic Boost-Glide Weapons;" "X-41 CAV (USAF/DARPA Falcon Program)," *Directory of U.S. Military Rockets and Missiles, Appendix 4: Undesignated Vehicles* (2009), <http://www.designation-systems.net/dusrm/app4/x-41.html>; this is similar to the result in Wright, "Research Note to Hypersonic Boost-Glide Weapons."
69. Phillips, "A Common Aero Vehicle."
70. Qinglin Niu, Zhichao Yuan, Biao Chen, and Shikui Dong, "Infrared Radiation Characteristics of a Hypersonic Vehicle Under Time-Varying Angles of Attack," *Chinese Journal of Aeronautics* 32 (2019): 867, <https://doi.org/10.1016/j.cja.2019.01.003>.
71. Using values for the CAV-L model gives somewhat lower lift but does not significantly change the results.
72. Candler and Leyva, "Computational Fluid Dynamics Analysis."
73. U.S. Government Accountability Office, "Hypersonic Weapons: DOD Should Clarify Roles and Responsibilities to Ensure Coordination across Development Efforts," GAO-21-378 (March 22, 2021): 13, <https://www.gao.gov/products/gao-21-378>; Steve Trimble, "Document Likely Shows SM-6 Hypersonic Speed, Anti-Surface Role," *Aviation Week*, March 12, 2020, <https://aviationweek.com/defense-space/missile->

- defense-weapons/document-likely-shows-sm-6-hypersonic-speed-anti-surface-role; Tyler Rogoway, “Navy To Supersize Its Ultra Versatile SM-6 Missile For Even Longer Range And Higher Speed,” *The Drive*, March 20, 2019, <https://www.thedrive.com/the-war-zone/27068/navy-to-supersize-its-ultra-versatile-sm-6-missile-for-even-longer-range-and-higher-speed>.
74. Tracy and Wright, “Modelling the Performance.”
 75. David Wright, Laura Grego, and Lisbeth Gronlund, *The Physics of Space Security* (Cambridge, MA: American Academy of Arts and Sciences, 2005), <https://www.ucsusa.org/resources/physics-space-security>. This equation assumes a single stage booster.
 76. U.S. Air Force, “AGM-86B/C/D Missiles,” Factsheet (August 2019), <https://www.af.mil/About-Us/Fact-Sheets/Display/Article/104612/agm-86bcd-missiles/>; U.S. Air Force, “AGM-129A Advanced Cruise Missile, Factsheet (n.d.), <https://www.af.mil/About-Us/Fact-Sheets/Display/Article/104543/agm-129a-advanced-cruise-missile/>; “AGM-158 JASSM,” *Airforce Technology*, July 5, 2013, <https://www.airforce-technology.com/projects/agm-158-jassm-standoff-missile/>; Sydney J. Freeberg, “Navy Warships Get New Heavy Missile: 2,500-Lb LRASM,” *Breaking Defense*, July 26, 2017, <https://breakingdefense.com/2017/07/navy-warships-get-new-heavy-missile-2500-lb-lrasm/>.
 77. Steve Trimble, “More ARRW Details Emerge as Congress, White House Add New Hurdles,” *Aviation Week and Space Technology*, July 14, 2021, <https://aviationweek.com/defense-space/missile-defense-weapons/more-arrw-details-emerge-congress-white-house-add-new-hurdles>.
 78. U.S. Air Force, “B-52H Stratofortress,” Factsheet (June 2019), <https://www.af.mil/About-Us/Fact-Sheets/Display/Article/104465/b-52h-stratofortress/>; U.S. Air Force, “B-1B Lancer,” Factsheet (September 2016), <https://www.af.mil/About-Us/Fact-Sheets/Display/Article/104500/b-1b-lancer/>; John A. Tirpak, “AFGSC Eyes Hypersonic Weapons for B-1, Conventional LRSM,” *Air Force Magazine*, April 7, 2020, <https://www.airforcemag.com/afgsc-eyes-hypersonic-weapons-for-b-1-conventional-lrsm/> reports the B1 may be able to carry up to 31 ARRWs, which would appear to give a total mass of 60,000–7,000 kg.
 79. “X-41 CAV (USAF/DARPA Falcon Program),” *Directory of U.S. Military Rockets and Missiles, Appendix 4: Undesignated Vehicles* (2009), <http://www.designation-systems.net/dusrm/app4/x-41.html>; Wright, “Research Note to Hypersonic Boost-Glide Weapons.”
 80. Woolf, *Conventional Prompt Global Strike*, and National Research Council, *U.S. Conventional Prompt Global Strike*.
 81. See Table 4.1 in National Research Council, *U.S. Conventional Prompt Global Strike*, 102–3.
 82. S. Fetter, “A Ballistic Missile Primer” (1990), <https://fetter.it-prod-webhosting.aws.umd.edu/sites/default/files/fetter/files/1990-MissilePrimer.pdf>. Note that we define the factor f differently than this reference.
 83. This value is somewhat lower than that of modern strategic reentry vehicles, since the MaRV is assumed to have fins and a nonzero angle-of-attack during reentry, although it need needs to generate less lift force during dive than a BGV, which dives from horizontal flight. At any point, the velocity angle is measured with respect to the local horizontal.
 84. Assuming $\beta = 7,500 \text{ kg/m}^2$ with $L/D = 2.6$ during glide and $L/D = -1$ to -2 during dive gives, for the Mach 5 case, 28.3 km altitude at the end of glide at and a dive range and time of 70 km and 62 s; for the Mach 9 case, the altitude at the end of glide is 36.4 km and the dive range and time are 143 km and 65 s.

85. Acton, “Hypersonic Boost-Glide Weapons.”
86. National Research Council, *U.S. Conventional Prompt Global Strike*, Appendix G; Acton, “Hypersonic Boost-Glide Weapons.”
87. Daniel Patrascu, “F-22 Raptor Pulls High Gs, Looks Cool Doing It,” *Autoevolution*, April 24, 2022, <https://www.autoevolution.com/news/f-22-raptor-pulls-high-gs-looks-cool-doing-it-186903.html>; U.S. Air Force, “F-16 Fighting Falcon,” Factsheet (September 2021), <https://www.af.mil/About-Us/Fact-Sheets/Display/Article/104505/f-16-fighting-falcon/>, states the F-16 can withstand nine g’s with a full load of fuel, but the body is larger than that of a BGV. National Research Council, *U.S. Conventional Prompt Global Strike* notes that new technologies can “withstand the effects of maneuvers up to 40 g’s.”
88. This insensitivity is in part because a longer ballistic phase at a given burnout speed will decrease the time the vehicle spends in glide and thus the duration of drag but will also result in a larger reentry angle and therefore require a sharper pull-up maneuver. This gives a larger velocity loss during pull-up, mitigating the effects of the shorter glide phase.
89. The MaRV typically requires a smaller L/D to put it on a steep dive since it begins reentry at a larger angle than the BGV. It could be designed to create higher lift if the goal was to increase the amount of maneuvering it could achieve during reentry.
90. Joseph Trivithick, “Army Delivers First Canisters to Its New Hypersonic Missile Battery but Won’t Say Where It’s Based,” *The Warzone*, May 19, 2021, <https://www.thedrive.com/the-war-zone/39851/army-delivers-first-canisters-to-its-new-hypersonic-missile-battery-but-wont-say-where-its-based>.
91. See for example, National Academies of Sciences, Engineering, and Medicine, *High-Speed, Maneuvering Weapons: Unclassified Summary* (Washington, DC: The National Academies Press, 2016), <https://doi.org/10.17226/23667>; Center for Strategic and International Studies, “Complex Air Defense: Countering the Hypersonic Missile Threat,” *Transcript*, February 9, 2022, <https://www.csis.org/analysis/complex-air-defense-countering-hypersonic-missile-threat-0>; Missile Defense Agency, “MDA Hypersonic Concept.”
92. Ivan Oelrich, “Cool Your Jets: Some Perspective on to Hying of Hypersonic Weapons,” *Bulletin of the Atomic Scientists* 76 (2020): 37–45, <https://doi.org/10.1080/00963402.2019.1701283>.
93. Zarchan, *Tactical and Strategic Missile Guidance*, 1: 272. This model works well for altitudes between 10 and 50 km.
94. Assuming instantaneous changes in glide altitude is a simplification that ignores the complicated dynamics of these maneuvers and the additional drag they would create. We assume these maneuvers are short compared to the time the vehicle spends gliding at the lower altitude, and that our estimate of the increased drag will be a reasonable lower bound, which shows the significant range reduction that can result from such a turn.
95. Since the vehicle is assumed to have enough vertical force to glide, this requires $\cos\theta \neq 0$.

Acknowledgements

The authors would like to thank Steve Fetter and Paul Zarchan for useful comments on parts of this work.

Disclosure statement

No potential conflict of interest was reported by the author(s).

Funding

DW was supported in part by the Laboratory of Nuclear Security and Policy at MIT and the Program on Science and Global Security at Princeton University.

ORCID

Cameron L. Tracy  <http://orcid.org/0000-0002-0679-8522>